PNAS RESEARCH ARTICLE | ANTHROPOLOGY ENVIRONMENTAL SCIENCES

The long-term expansion and recession of human populations

Jacob Freeman[a,b,1], Erick Robinson[c,d,e], Darcy Bird[f,g], Robert J. Hard[h], Raymond P. Mauldin[i], and John M. Anderies[e,j]

Edited by George Milner, The Pennsylvania State University-University Park Campus, University Park, PA; received August 5, 2023; accepted January 31, 2024

Over the last 12,000 y, human populations have expanded and transformed critical earth systems. Yet, a key unresolved question in the environmental and social sciences remains: Why did human populations grow and, sometimes, decline in the first place? Our research builds on 20 y of archaeological research studying the deep time dynamics of human populations to propose an explanation for the long-term growth and stability of human populations. Innovations in the productive capacity of populations fuels exponential-like growth over thousands of years; however, innovations saturate over time and, often, may leave populations vulnerable to large recessions in their well-being and population density. Empirically, we find a trade-off between changes in land use that increase the production and consumption of carbohydrates, driving repeated waves of population growth over thousands of years, and the susceptibility of populations to large recessions due to a lag in the impact of humans on resources. These results shed light on the long-term drivers of human population growth and decline.

human population | human ecology | demographic transitions | radiocarbon

Significance

A revolution in archaeological research now reveals that human populations grew exponentially during periods of the Holocene, disrupted by periods of recession. This deep history of long-term population expansion and recession requires an explanation. In this paper, we propose an explanation that unifies the population growth dynamics of human societies across environments. We argue that human populations face tradeoffs between innovations that massively scale-up human well-being and unintended punctuated recessions. The recessions occur when innovation slows and competition suddenly degrades key resources. The theory and data analysis provide a framework for understanding diverse trajectories of human population growth. Explaining this diversity in the past provides context for understanding the factors that may impact population dynamics in the coming centuries.

The last 20 y have witnessed a revolution in the ability of archaeologists to describe long-term patterns of population growth (e.g., refs. 1–17). This research explosion demonstrates two general findings. First, most regions of the world display long periods of positive, exponential-like growth. For example, Zahid and colleagues illustrate a similar rate of exponential population increase from 12,000 to 6,000 cal BP among archaeological regions inhabited by hunter-gatherers and agriculturalists (7). More widely, Freeman and colleagues document that human populations experienced correlated, exponential-like growth, regardless of technological and climate differences, throughout the Holocene (9). These correlated patterns suggest that a similar underlying process of population growth operated across different types of physical environments and human economies during the Holocene. Second, following periods of expansion, human populations often display oscillations and the magnitude of these oscillations vary over space and time (e.g., refs. 2, 8, 10–12, 16 and 18–20). For instance, in NW Europe, human populations experienced a sustained expansion beginning with the spread of agriculture followed by a recession of population for hundreds of years (2). Similar "expansions and recessions" occur worldwide (21).

The above findings suggest two fundamental questions. i) What mechanisms enable human populations to often display positive, exponential-like growth over thousands of years, and ii) why do some regions display more stability (less violent oscillations) than other regions? To help answer these questions, we use controlled comparisons of large datasets of radiocarbon ages associated with human activity (e.g., ref. 22) and data on changes in the production of resources to test an Adaptive Capacity Tradeoff Hypothesis. This hypothesis synthesizes the basic insights of many models of long-term population growth (e.g., refs. 23–35), providing a potential explanation for both positive, exponential-like growth over a few thousand years and variation in population stability. Our results contribute to a general theory of innovation-driven demographic transitions in human societies and suggest that innovations, such as the adoption of intensive agriculture, that massively increase human well-being in the shorter-run require larger recessions in the longer-run due to lags in the impacts of competition for resources on ecosystems.

Adaptive Capacity Tradeoff Hypothesis

Following the strategy of Cohen (23), we use a cartoon model to help illustrate a general Adaptive Capacity Tradeoff. This model describes four key processes in human populations: The amplifying feedback of population growth, the balancing feedback of competition, population escapes through innovations that impact the production of resources, and, finally, the delayed impact of human populations on ecosystems.

Author contributions: J.F. and E.R. designed research; J.F., D.B., R.J.H., R.P.M., and J.M.A. performed research; J.F. analyzed data; and J.F., E.R., D.B., R.J.H., R.P.M., and J.M.A. wrote the paper.

The authors declare no competing interest.

This article is a PNAS Direct Submission.

[1]To whom correspondence may be addressed. Email: jacob.freeman@usu.edu.

This article contains supporting information online at https://www.pnas.org/lookup/suppl/doi:10.1073/pnas.2312207121/-/DCSupplemental.

Published March 11, 2024.

All four processes occur, though not always in the same model, in a class of formal models called Malthus–Boserup models of human population growth (e.g., refs. 23, 24, 29–34, and 36). To capture these processes, we build on a modified version of the logistic model (37),

$$\dot{p}(t) = rp(t) - \frac{Sp(t)^2}{K}, \quad [1]$$

where $\dot{p}(t)$ is the change in human population in a given area at time t; r (1/time) is the per capita rate of population growth in the absence of environmental or social constraints (i.e., the "intrinsic" growth rate); S (1/time) is the cost of social integration, $0 < S \leq 1$, and K is the maximum population that a given area can support based on the productivity of the resources used by humans. In Eq. **1**, rp captures the tendency of a population to increase exponentially [(38), amplifying feedback], and $-\frac{Sp(t)^2}{K}$ captures the dampening effect of competition for resources on population growth [(38), balancing feedback]. If S were zero, then human populations could achieve the level of social integration necessary to exploit resources at arbitrarily large scales. The same effect occurs by making K arbitrarily large. The key feature of Malthus–Boserup models is a description of the race between environmental constraints imposed by a fixed K (Malthus) and endogenous innovations in technology and land use that increase K over time (Boserup).

A critical insight of previous models is that innovations in the production of resources may be driven by population pressure (24, 30, 31, 34, 36, 39). Population pressure is defined as the minimum tolerable fitness (well-being) greater than the fitness necessary for a population to replace itself. Whenever per capita fitness crosses the minimum tolerable threshold, populations receive signals of intolerable competition for key resources that provide incentives to adopt alternative forms of social organization and infrastructure for producing food. However, it is not well understood whether innovations occur as a linear function of the background rate of cultural evolution (34), continuously ratcheting a population higher and higher, or whether innovations in the production of food diminish in their effectiveness over time as landscapes become transformed and occupied (23, 30, 31, 36). Recent evidence among hunter-gatherers suggests that changes in resource extraction that raise K may, in fact, saturate over time (40). Two problems arise: i) over hundreds of years, innovations that up-scale food production, and, thus, population to a higher equilibrium level only provides temporary increases in well-being (e.g., refs. 24, 25, 30, and 31). This occurs because population growth fills-in the new niche and results in the system re-entering a state of population pressure. ii) More interestingly, over hundreds to thousands of years, populations may hit an innovation ceiling, becoming so specialized that individuals invest in making their current systems more efficient and more entrenched rather than innovating (29, 31, 40).

To capture the up-scaling of a population system to a higher K and the effect of an innovation ceiling, we first divide both sides of Eq. **1** by $p(t)$ to calculate the mean per capita fitness, f of a population:

$$f \equiv \dot{p}(t)/p(t) = r - \frac{Sp(t)}{K}. \quad [2]$$

Next, we write the change in environmental constraints on a population due to the productivity of resources as a function of time,

$$K_i(t) = A_i - B_i p(t-d) + C, \quad [3]$$

where A_i describes the effect of human-made infrastructure on the productivity of resources in a set of ecosystems over the climate controlled resources available to culturally unaided primates (C). For example, the climate-controlled net primary productivity of terrestrial ecosystems impacts the population density of ethnographically recorded hunter-gatherers, agriculturalists, and modern countries in the same way (41). However, holding net primary productivity equal, increasing specialization on agriculture results in much higher population densities (41, 42) due to the augmentation of productivity on the landscape by individuals and communities. B_i describes the relationship between the productivity of resources and population density for strategy i; and $(t-d)$ defines the delay of a population's impact on resources.

In the standard continuous time logistic model, a population always displays a smooth convergence to equilibrium. Oscillations in the dynamics of human population, as with other species, only occur in the presence of delays initiated by predator–prey interactions (33). Here, to create a general framework for comparison, we use a simple delay function to capture the effect of a lag between harvest pressure on prey and prey response (37). In real social–ecological systems, the delay may occur because ecosystems have the capacity to withstand and respond to harvest pressure and humans adjust their behavior to dampen resource degradation. For example, in the classic logistic model formulation, if a population adopts shifting rice agriculture, it takes time for a population to grow and fill-in potential places where shifting agriculture produces well. Once these areas become occupied, then mature vegetation cover declines and farmers experience declines in surplus production and, thus, per capita fitness. However, in real systems farmers may adjust their behavior to such a situation by spending more time weeding their gardens and increasing the tempo of garden rotation, delaying a decline in the output of agricultural surplus. Together, both processes can create a delay in the impact of increasing population density on surplus production.

Finally, we add an "if, then, else" function to capture the process of innovation stimulated by population pressure that leads to transitions in the production of resources. If $f_{min} < f$, then $K_1(t)$, else $K_2(t)$. For convenience, we study two functions, $K_1(t)$ and $K_2(t)$, to capture the demographic transition dynamics of the model driven by an innovation in productive capacity. A demographic transition refers to a situation in which population density and the mean fitness of a population shift from a negative to a positive and then back to a negative relationship. Note that the transition from $K_1(t)$ to $K_2(t)$ captures an "easy" innovation in productive capacity, whereas the lack of a K_3 denotes an innovation ceiling. We hold C, r, and B_i constant and study how changes in A, S, and d impact the system. Here, we assume that $A_1 < A_2$ and $B_1 > B_2$. We make these assumptions to simulate the effects of humans adopting infrastructures that allow them to extract more resources from ecosystems, though at the cost of greater impacts on ecosystems in the future.

Model Dynamics. Fig. 1 illustrates the dynamics of the model for three experiments. Fig. 1 *A* and *B* document the following: In the absence of a delay, a larger innovation in the productivity of resources generates larger, longer demographic transitions and a smooth transition into a higher equilibrium population density. For instance, in Fig. 1*B*, at about 20 generations, the population increases upward from the A = 0 curve (no innovation, baseline population model). The length of increase and equilibrium population displayed after the 20 generation mark is determined by the positive value of $A = A_2 - A_1$.

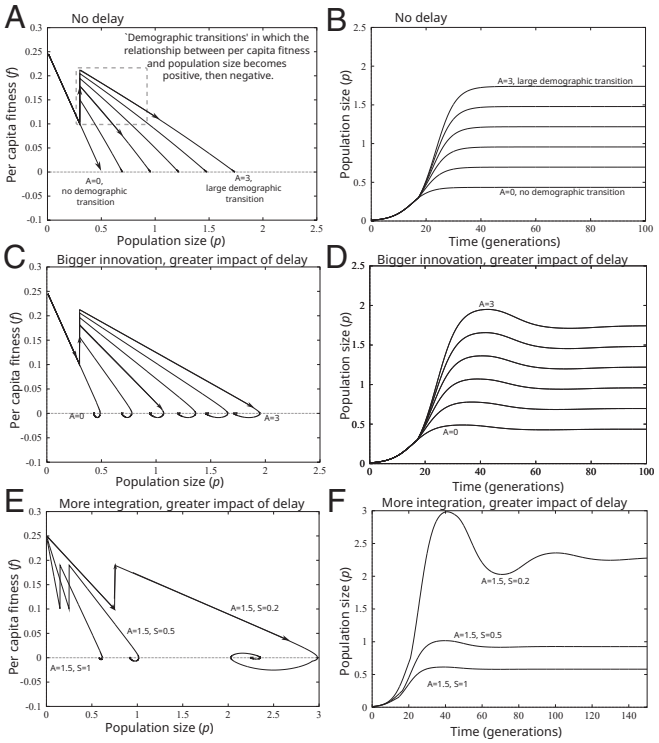

Fig. 1. (*A*) Per capita fitness vs. population density, illustrating demographic transitions as a function of *A*, with all other parameters held constant: $r = 0.25$ (per generation which is equivalent to roughly 1-2% annual growth rate depending on generation times), $S = 0.5$ (per generation), $d = 0$, $C = 1$, $A_1 = 0$, $B_1 = 0$, $B_2 = -0.25$, and $A_1 < A_2$. As *A* increases, the productivity of resources increases. (*B*) Illustration of population dynamics over time. The $A = 0$ curve illustrates population dynamics with no demographic transition due to the adoption of infrastructure that increases productivity. Higher values of *A* result in larger and longer demographic transitions. (*C*) Same as graph A but with delayed impact ($d > 0$) and other parameters held constant as above. The delayed impact of human populations on the resource stock results in an overshoot and recession displayed by the hook shape of each curve. (*D*) Population dynamics over time with a delay. As *A* increases, the overshoot and recession intensifies. (*E*) Per capita fitness vs. population density as *S* varies. All parameters are the same as above and $A = 1.5$. As *S* increases, equilibrium population density increases, the length of the demographic transition increases, and population stability decreases. (*F*) Population dynamics over time for different *S*.

Fig. 1 *C* and *D* replicate the figures above, except that now population size has a delayed effect on the productivity of resources. In panel *C*, again, a larger innovation in the productivity of resources generates a longer demographic transition. However, the larger innovation also magnifies the impact of the delay. This is denoted by the hooked shape of the curves in Fig. 1*C*; the larger hooks reaching lower negative per capita fitness. Fig. 1*D* illustrates the expansion–recession pattern over time. The population expansion and recession occurs because the combination of a greater increase in energy extraction and a delay weakens the balancing feedback of competition on population growth. Thus, growth races ahead of competition until the resource constraint suddenly hits and per capita fitness turns negative. This occurs until the amplifying feedback of growth once again balances competition and the system enters equilibrium.

Finally, Fig. 1 *E* and *F* replicate panels *C* and *D*; however, we hold *A* equal and change the costs of social integration, *S*. Fig. 1*E* illustrates that as *S* increases, the length of the demographic transition, equilibrium population size, and population recession become larger. This last dynamic is illustrated over time in Fig. 1*D* by the sudden uptick in population growth around 20 generations and the increasingly humped shape of the curve as *S* increases. Again, the innovation-driven overshoot occurs because the lower cost of social integration weakens the balancing feedback of competition for resources. Consequently, population growth races ahead of competition until the population hits a sudden "competition cliff." At this point, the balancing feedback overpowers growth, population declines, and the system eventually enters equilibrium.

In summary, both the long-term population expansion and overshoot-recession pattern documented in many archaeological regions require an explanation (e.g., refs. 4, 7, 9, 19, 21, and 43). We propose that these patterns result from i) waves of "demographic transitions" as populations increase their ability to extract resources from ecosystems over time; ii) however, given the potential delays in the negative impacts of human populations on ecosystems, a greater ability to augment the productivity of ecosystems and/or a lower cost of social integration results in longer periods of expansion and rapid recessions when populations hit an innovation ceiling. Greater investments in constructing highly productive niches create greater adaptive capacity *now*, generating longer and more robust population growth, but results in population decline and pain later, rather than a smooth transition into an equilibrium. This argument suggests three expectations in the context of deep time population dynamics.

First, population expansion over thousands of years results from increases in the ability of populations to extract more resources from ecosystems, especially shifts toward the production of energy-dense carbohydrates that require less area per person. Second, periods of positive growth are longer in regions where populations adopted more productive economies, like agriculture, than in regions where populations focused resource extraction on hunting and gathering techniques. Finally, population recessions should be larger in regions where populations adopted agriculture and had greater levels of social integration (e.g., through large ceremonial centers). These last two expectations follow from the model dynamics discussed above. Larger innovations in the productivity of resources and higher levels of social integration weaken the balancing feedback of competition, leading to larger overshoots and recessions, if populations approach an innovation ceiling. If populations did not approach an innovation ceiling, then populations would simply grow continuously with no oscillations (e.g., ref. 34).

Results

To evaluate the above expectations, we conduct comparisons at two scales (Fig. 2). First, we conduct a controlled comparison of the Middle Mississippi River Valley and Central Texas in N. America. This controlled comparison assesses the population dynamics of regions with similar ecosystems (grassland to wooded savanna), abundant evidence of changes in resource production over the last 3,500 y, and significant differences in social–ecological adaptations. People in the Middle Mississippi River Valley adopted agriculture and, eventually, large centers of population aggregation that should have lowered the costs of social integration [e.g., Cahokia (44, 45)]. The people of Central Texas intensified their production of wild resources, especially wild tubers and bulbs over the last 3,500 y, and remained mobile hunter-gatherers with little evidence of large-scale ritual centers. Second, we compare eight ArchaeoGlobe Regions (46) from the Lower 48 US states. This larger comparison allows us to use estimates of changes in land use made in the ArchaeoGlobe

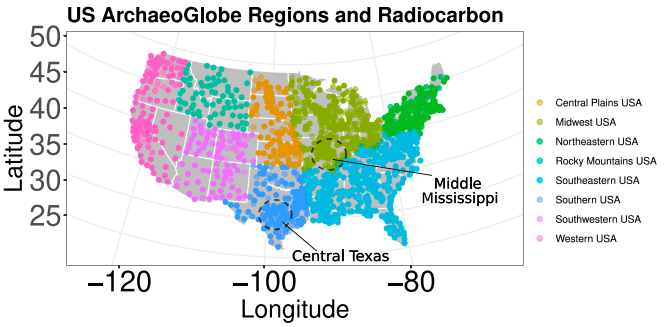

Fig. 2. Map of radiocarbon data from the eight ArchaeoGlobe Regions (Albers equal area projection) used in this study. Dashed circles highlight the Central Texas and Middle Mississippi River Valley case studies.

dataset to evaluate the presence of adaptive capacity tradeoffs (i.e., larger innovations in production due to agriculture create longer periods of increases in fitness but require larger recessions) among regions that adopted agriculture to various degrees over the last 3,500 y.

Scale 1. Fig. 3 compares the change in population density (*A* and *B*), individual fitness (*C* and *D*), and resource extraction technology and diet (*E* and *F*) over time in the Middle Mississippi River Valley and Central Texas. In the Middle Mississippi River Valley and Central Texas, we track changes in resource production using stable isotopes associated with human bone from 354 individuals (Mississippi Basin) and 78 individuals (Central Texas). Changes in $\delta^{15}N$ allow us to track the trophic position of consumers, with higher values indicating more consumption of protein (e.g., American bison, deer, and/or fish) and lower values indicating less consumption of these resources. Further, in the Middle Mississippi River Valley, we use an index of cultigens relative to nuts to estimate changes in the specialized production of carbohydrates from domesticated plants (14). In Central Texas, we use the ratio of large earth oven middens that result from the repeated baking of wild roots to small cooking features as an estimate of specialization in the production of carbohydrates. In both cases, the higher the index, the more effort people invested in producing and consuming energy-dense carbohydrates that require longer processing times.

In both regions, we observe population curves that increase in a non-linear way over 3,500 y, with a peak at about 800 cal BP (Fig. 3 *A* and *B*). Although both cases display a curve-linear increase from 3,500 to 800 cal BP, this growth is distributed differently. In the Middle Mississippi River Valley, populations experienced a positive per capita growth rate, on average, for 23.3 consecutive 30-y generations. For example, the mean and 95% CI of per capita growth remain positive in the Middle Mississippi from 2,300 to 800 cal BP (see the dashed box on Fig. 3*C*). Conversely, Central Texas populations only display positive per capita growth, on average, for 7.42 consecutive generations, and the 95% confidence envelop of per capita growth is much more variable between 2,300 and 1,400 cal BP (compare dashed boxes on Fig. 3 *C* and *D*). Finally, the exponential-like increase in population, in both regions, associates with a step-wise increase in the production of energy-dense carbohydrates and a significant decline in protein consumption near the peak of each curve. In Fig. 3*E*, $\delta\ ^{15}N$ values remain stable between Periods 1 and 2; however, the cultigen index increases from 0.027 to 0.19 from Period 1 to 2. From period 2 to 3, we observe a significant decrease in $\delta\ ^{15}N$ values (W = 1,353, *P*-value < 0.05) and, again, an increase in the cultigen index from 0.19 to 0.77. During Period 5, when the population of the Mississippi River Basin declines, the cultigen index decreases to 0.61, and we observe a significant increase in $\delta\ ^{15}N$ values (W = 2473.5, *P*-value < 0.05). A very similar pattern occurs in Central Texas (Fig. 3*F*). $\delta\ ^{15}N$ values remain unchanged from Period 1 to 2, but the midden index increases from 0.27 to 0.31. Near the peak of population during Period 3, we observe a major increase in the midden index to 0.51 and a significant decline from period 2 to 3 in $\delta\ ^{15}N$ values (W = 187.5, *P*-value < 0.05). Finally, as the population curve declines during Period 4, we observe a decrease in the midden index to 0.11 and a significant increase in $\delta\ ^{15}N$ values (W = 22.5, *P*-value < 0.05).

In summary, our controlled comparison presents evidence consistent with expectations. Both regions experienced population growth over thousands of years associated with step-wise increases in carbohydrate production and a decline in $\delta\ ^{15}N$ values near peak population densities. Further, greater commitment to agriculture and larger-scale social integration in the Middle Mississippi River Valley associates with longer periods of positive per capita growth but a more dramatic population recession. The agricultural system achieved exponential expansion through

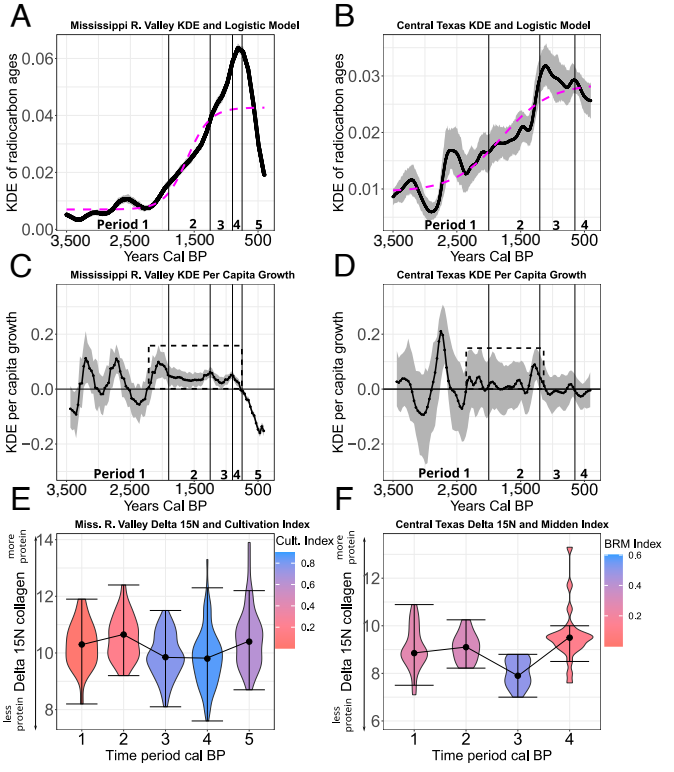

Fig. 3. Time-series of population, resource extraction technology, and diet in the Middle Mississippi River Basin and Central Texas. (*A* and *B*) Mean kernel density estimates (KDE) and 95% confidence envelope of 200 KDE simulations (gray shading). (*C* and *D*) Per capita growth rates of mean KDE's in the Middle Mississippi River Basin and Central Texas. Gray shading is the 95% confidence envelope of simulated KDE growth rates. (*E* and *F*) Violin plots of $\delta\ ^{15}N$ values from 354 individuals in the Middle Mississippi River Basin and 78 in Central Texas. Each violin plot is shaded by the median cultigen index (Mississippi) or midden index (Texas) during cultural historical time periods (*Data and Methods*). The change in color of the violin plots indicates changing technology over time from less (red) to more to intensive carbohydrate processing (blue). The black dots indicate the median of the distribution and illustrate the changing physiological impact of a shift to more carbohydrate production. These two lines of evidence indicate innovative processes that sequentially increased K (i.e., moving from K_1 to K_2 in our model). Error bars are shown at 95 % of the distribution.

successive demographic transitions in which per capita growth remained positive until the population hit a demographic cliff at 800 cal BP, declining for 300 y. The hunter-gatherer system achieved exponential-like growth via moderate periods of positive per capita growth interspersed by many short periods of negative per capita growth. In Central Texas, populations declined after 800 cal BP less rapidly and severely. In both cases, population decline after 800 cal BP associates with an increase in protein consumption and decline in carbohydrate production, as we would expect in a dynamic predator–prey system as human population decline released pressure on resources and ecosystems recovered.

Scale 2. Recall that we expect larger innovations in productive capacity to generate longer demographic transitions but also require larger population recessions, if an innovation ceiling occurs (as illustrated in the case studies above). In Fig. 4, we use the presence of extensive agriculture over hunting and gathering and intensive agriculture in addition to extensive agriculture as a proxy for larger innovations in the productivity of resources among eight ArchaeoGlobe regions. Partly consistent with expectations two and three, Fig. 4 illustrates that regions practicing agriculture experience longer periods of consecutive positive per capita growth than populations practicing hunting and gathering. In particular, the large increase in energy extraction afforded by intensive agriculture leads to longer periods of population expansion. Similarly, investing in extensive and intensive agriculture leads to more extreme recessions (estimated by the minimum negative per capita growth experienced in a region). For example, just as with the comparison of the Middle Mississippi and Central Texas, populations experienced extreme recessions in the Southwest and Midwest ArchaeoGlobe regions around 800 cal BP after adopting intensive agriculture in the preceding centuries. Conversely, the Western ArchaeoGlobe region, dominated by hunter-gatherer adaptations, experienced more frequent and much smaller recessions (*SI Appendix*, Part III).

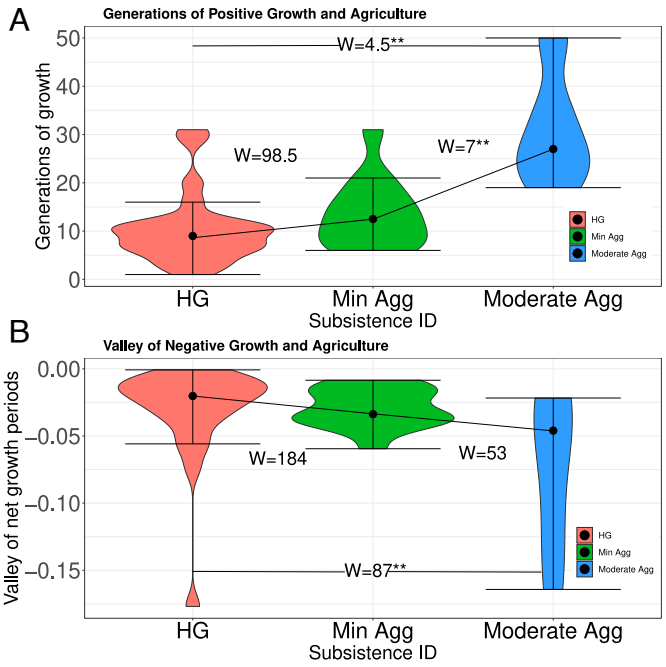

Fig. 4. The relationship between length of population expansion and severity of subsequent population recession. (*A*) Length of consecutive positive per capita growth rates among ArchaeoGlobe regions by subsistence land use categories. HG = hunting, gathering, and fishing. Min. Agg = extensive agriculture only. Moderate Agg. = extensive and intensive agriculture land use types. (*B*) The lowest per capita growth rate associated with periods of negative growth in the eight ArchaeoGlobe regions. HG = hunting, gathering, and fishing. Min. Agg = extensive agriculture only. Moderate Agg. = extensive and intensive agriculture land use types. *A* and *B* together suggest that the longer the growth phase, the more intense the subsequent recession.

Discussion

The proliferation of open access archaeological data and synthesis of large radiocarbon datasets (e.g., refs. 2, 9, 10, 18, 22, and 47–49) is changing archaeology. Over the past 20 y, two dominant patterns have emerged from an analysis of these datasets. First, human populations often display exponential-like growth over a few thousand years. Second, following these periods of expansion, human populations sometimes display recessions and oscillations. In this paper, we developed and began to evaluate a general explanation for these patterns. Human populations face an unintended Adaptive Capacity Tradeoff. Large innovations in the ability to extract resources from ecosystems, such as the adoption of intensive agriculture, generate large and consistent gains in well-being in the shorter-run. However, such large innovations require populations to "pay" with large declines in well-being—population recessions—in the longer-run. Mechanistically, the transformation of social–ecological landscapes causes a delay in the feedback from resource conditions to decisions about investments in capital and innovation. These delays may lead to a doubling down on existing forms of production rather than innovations, potentially producing population recessions.

Our analysis is partly consistent with the Adaptive Capacity Tradeoff explanation at two scales. First, comparing the Middle Mississippi River Valley and Central Texas reveals that populations in both regions increased their use of energy-dense carbohydrates in a step-wise process over time. This increased production and consumption of carbohydrates associates with persistent population growth, waves of increases in mean fitness over 3,000 y, and a marked decline in protein consumption very near peak population density in each region (Fig. 3). Further, the evolution of the agricultural system (Mississippi River Valley) displays longer periods of consecutive positive per capita growth and a very large final population recession. The hunter-gatherer system displays shorter periods of positive per capita population growth interspersed by shorter periods of negative growth. These patterns are consistent with model dynamics indicating that large innovations in resource productivity, for example, due to agriculture, lead to the capacity to sustain positive per capita growth rates now, but also introduces delays that require larger population declines in the future. Second, we observe similar dynamics among the eight ArchaeoGlobe regions of the modern US. More transformation of land use to include extensive and intensive agriculture results in longer periods of positive per capita growth and more severe population recessions.

Our study raises important questions for future research and understanding when and why human populations display successive waves of expansion and periodic recess. First, our approach focuses on general systems dynamics as opposed to individual decisions in the context of life history theory (43). Ultimately, we need a multi-scalar theory of human population growth that explains both the long-term expansion of populations over thousands of years and shorter-term fluctuations. This multi-scalar theory informed by deep time archaeological data will be essential for understanding the long-term implications of the demographic dynamics humans are currently experiencing. The key to understanding long-term population expansion is an

ability to explain why rates of innovation and people's affinity for adopting innovations change over time. Certainly, this will require understanding both systems dynamics and how individual preferences for novelty shift with changing demographic and social circumstances.

Second, our analysis focused on two scales. The first was a controlled comparison of two regions with distinct economies and culture histories. This scale of analysis links to a long-standing interest in reorganization/collapse in archaeology and beyond. For instance, in the Middle Mississippi River Valley and surrounding area, researchers have long proposed that climate change and/or social stresses were integral components of the expansion of population around 1,000 cal BP, nucleation of populations in centers such as Cahokia, and then the decline of these centers and population around 770 cal BP (17, 50–52). Our point here is not to provide an alternative to such explanations. Rather, we argue that in many cases, "population collapses" are notable recessions of the carrying capacity of a region that has its antecedents not simply in the decades and centuries prior, but in the transformation of human infrastructure systems over millennia. Given that human populations embed within and create multiple interacting complex adaptive systems, the immediate antecedents to such recessions will always have a unique path dependence and confluence of local factors. But the general pattern driving growth and creating a vulnerability to recessions is the same, we argue, across regions with cultural evolutionary histories as different as Central Texas and the Middle Mississippi River Valley. A comparison of dozens of cases at this scale will help evaluate the ultimate merit of this hypothesis.

The second scale of analysis focused on comparing ArchaeoGlobe regions from within the modern US political boundaries. This scale of analysis averages over many different ecosystems and cultural histories, even within any one ArchaeoGlobe region. For example, the Western US and Northern Rocky Mountains were dominated by hunter-gatherer land use strategies throughout the Holocene. However, hunter-gatherer land use, just as in Central Texas, changed over time and in different ways across these regions. Thus, future research should document the different trajectories of hunter-gatherer population change and compare these trajectories with areas where people adopted agriculture. Further, no doubt many North American archaeologists may point to the different climates across the continent as a key driver of population growth patterns. As evidenced by the inclusion of climate in Eq. **2**, we suspect that climate plays an important role, potentially impacting the process of integrating innovations in food production into extant social and economic patterns. Clearly, more work is needed to refine archaeological chronologies to the resolution necessary to document and understand the role of climate in the process of innovations, or lack thereof, in food production.

Third, we qualitatively suggest that the Middle Mississippi River valley developed a lower cost of social integration than Central Texas, and the same for the US Southwest, Midwest, and Southeast relative to the other ArchaeoGlobe regions at a larger scale. The evidence for this is that, in these regions, people developed more integrative ritual centers and widespread iconography associated with centers (e.g., Cahokia, Chaco Canyon, Hohokam platform mounds) (e.g., refs. 44, 45, and 53–55). Thus, we suggest that S became lower over time within these systems, supercharging population overshoots. However, much more work is needed to measure S, archaeologically. We need better theory that connects the costs of social integration with material remains and quantitative time-series of relevant archaeological remains.

Importantly, shared rituals and centers that lower the costs of social integration (e.g., build trust, social capital) always do so for some (in-groups) but not others (out-groups). Thus, social mechanisms, such as increases in the scale of shared rituals, may also associate with more warfare, and disentangling these effects on population requires more work. For example, Kondor and colleagues recently proposed an agent-based model to help explain expansion and recession dynamics in Mid-Holocene Europe (18). They conclude that a model with social conflict (war) better reproduces fluctuating population dynamics than a model that relies on climate perturbations to agricultural carrying capacity alone. Although on the surface quite different from our approach, ultimately the expansion–recession patterns in their model are caused by delays between population growth and the density-dependent feedback of direct competition for resources and warfare. Future research needs to investigate the interaction of changes in the productive capacity of a resource due to innovations, integrative social structures that impact the costs of social integration, and conflict between in and out-groups.

In the end, we argue that the long-term expansion of human populations and recessions may be interrelated. Innovations in the production of food, especially carbohydrate-dense plants, drive waves of long-term positive growth over thousands of years. However, innovations that provide adaptive capacity now also generate long-term trajectories of population growth that transform landscapes. Such landscape transformations may create delays in the effect of density-dependent competition for resources and result in eventual large population recessions. Particularly important in this context is the role of incremental innovations in social integration and productive capacity that only raise a region's carrying capacity a little (Central Texas) vs. large innovations that raise a region's potential carrying capacity a lot (Mississippi River Valley). Large increases in integration and productivity where human impacts on ecosystems have a delay lead to a competitive cliff. Populations experience larger scale and longer-term expansion, but at the expense of more painful population recessions (see also refs. 10 and 11). Such dynamics in population systems provide one empirical example of the tradeoff in complex adaptive systems between suppressing variability (i.e., learning) to gain productivity, perhaps for a long time, but at the expense of greater fragility to slow environmental change in the future (e.g., refs. 11 and 56–59).

Data and Methods

The formal model in Eqs. **1**–**3** was analyzed numerically in XPPAUT (60) (*SI Appendix*, Part I). All other data are available at ref. 61. To evaluate the Adaptive Capacity Tradeoff Hypothesis, we used previously published data from the Middle Mississippi River Valley and Central Texas (Fig. 2) (14, 62–66). We divided the two above archaeological cases into cultural historical phases identified by archaeologists in each region. In the Middle Mississippi River Valley, which includes the American Bottom, Illinois River Valley, and sites into Missouri, we divided the sequences into Middle Woodland, Early Late Woodland, Late Late Woodland, Mississippian, and Oneota Phases. Fig. 3*E* compares the distribution of isotope values by each cultural historical phase ($n = 354$ individuals), and we used a Mann–Whitney U test to evaluate the null hypothesis that the distribution of isotope values between consecutive phases comes from the same distribution. We consider a P-value of less than 0.1 as sufficient evidence to reject the null hypothesis. We focus here on changes in $\delta^{15}N$, which allow us to track the trophic position of consumers. Higher values potentially indicate more consumption of large to medium-sized animals and/or more fish, and lower values potentially indicate less use of these resources (*SI Appendix*, Part II).

Once we developed a database of human bone isotopes in the Middle Mississippi, we used an index of nuts to cultigens found in archaeological sites

in this region over the last 5,000 y cal BP published by Milner and Boldsen (14). We selected sites that overlap geographically with the sites from which the isotope data were recorded, and we then calculated the median cultigen index by each cultural historical phase. Note that our results do not change if we use the whole dataset, which encompasses sites from Eastern N. America more broadly (*SI Appendix*, Part II). The cultigen index provides an estimate of the production and use of small domesticated seeds, such as amaranth and maize, relative to nuts higher in protein and fats. The index is calculated as the percentage of cultigens found in site ethnobotanical samples divided by nuts plus cultigens. In general, the domesticated seeds provide lower returns per person hour than nut resources (67). Thus, higher index values indicate more production and use of lower return rate carbohydrates with less protein and fat.

In Central Texas, we divided the sequence into four phases: Early Late Archaic, Terminal Late Archaic, Early Late Prehistoric (Austin Phase), and Late Late Prehistoric (Toyah Phase). Fig. 3*F* compares the distribution of isotope values by each cultural historical phase ($n = 78$ individuals), and we used a Mann–Whitney U test to evaluate the null hypothesis that the distribution of isotope values between successive phases comes from the same distribution. To track the production of carbohydrates in Central Texas, we used a database of 303 dated fire-cracked rock features that resulted from suspected earth oven cooking (40). Earth ovens are a general cooking technology; however, substantial evidence indicates that the remains of such ovens in Central Texas were used to bake root species for prolonged periods of time (e.g., refs. 40 and 68–70). We ran a cluster analysis of the features, identifying two clusters of feature size: those that cluster around 1 square meter and those that cluster around 100 square meters in surface area. Surface area serves as an estimate for the size of cooking oven and the number of times a cooking feature was reused, generating more fire-cracked rocks (*SI Appendix*, Part II). Thus, the more that foragers in Central Texas baked roots in the same location, the larger middens should have become. To estimate commitment to the production of root species, we calculated an index of large middens divided by the number of large middens plus small features. The higher this index, the more frequently foragers bulk processed roots in the same locations. The smaller the index, the more small, unique cooking sites foragers created on the landscape.

To reconstruct the population dynamics of the Middle Mississippi River Valley and Central Texas, we used archaeological radiocarbon. We pulled and analyzed 3,167 archaeological radiocarbon ages from Bird et al. (22) that overlap with the geographic distribution of sites with human bone isotopes discussed above, and we used the 1,762 radiocarbon ages published from Central Texas by Freeman et al. (40). We used the R package rcarbon to construct Kernel Density Estimates (KDEs) to estimate changes in population in each region over the last 3,500 y cal BP (71) (*SI Appendix*, Part II). While radiocarbon records are subject to potential biases, archaeologists have developed models and techniques to control for the biases of sampling intensity, preservation, and the non-linear radiocarbon calibration curve (e.g., refs. 4, 5 and 71–76). To help address these concerns, we constructed mean KDEs in each region by running 200 simulations with a bandwidth of 50 and then calculated the mean of the 200 KDEs. We then summed the KDEs into 30 y bins. Both of these procedures smooth the KDE to capture the long-term trend over time and reduce intra-generational fluctuations over shorter time-scales induced by calibration and/or biases introduced by site over-sampling (*SI Appendix*, Part II for alternative methods). Further, we constructed these KDEs to 200 cal BP and then trimmed the sequences to 410 cal BP. We end the sequences at 410 cal BP to avoid biases potentially associated with a lack of radiocarbon dating of material remains in N. America after European manufactured items become common and, potentially, useful to date archaeological sites (*SI Appendix*, Part II, *Edge Effects and Taphonomy*). In both cases, we are conservative and do not use a global taphonomic adjustment proposed by (77) because the adjustment introduces complexity and uncertainty into the data (*SI Appendix*, Part II, *Edge Effects and Taphonomy*). We used Intcal2020 to calibrate the radiocarbon ages (78).

We analyzed the mean KDE in two ways. First, we fit a logistic model to capture the trend over time in the mean KDEs. We use the logistic model because the Adaptive Capacity Tradeoff Hypothesis proposes that population growth over thousands of years follows innovations that, at first raise a population's limit a lot, but then display diminishing returns, leading to a slowing of increases in a population's limit as an innovation ceiling is approached. Second, we calculated the per capita growth rates of the mean KDEs as $\ln(MKDE_{t+1}/MKDE_t)$. We then calculated the number of consecutive generations that each case displayed positive per capita growth, and we recorded the minimum and maximum per capita growth rates in each period of consecutive growth or decline.

To scale our analysis up to ArchaeoGlobe regions, we analyzed archaeological radiocarbon ages documented from eight ArchaeoGlobe regions in the lower 48 contemporary United States. We did this by joining archaeological radiocarbon synthesized by Bird et al. (22) with ArchaeoGlobe shape files. We then constructed KDEs for each region following the same procedures outlined above. Next, we integrated ArchaeoGlobe estimates of land use (46) with the mean KDE data. In particular, ArchaeoGlobe uses a consensus of expert opinions to estimate how widespread types of land use were at 1,000 y intervals. In our cases, land use types include hunting, gathering, and fishing, extensive agriculture, intensive agriculture, and urbanism (or a high degree of settlement nucleation). We assume, based on ethnographic evidence (e.g., ref. 41), that agricultural land use, on average, has a higher productive potential than hunting and gathering land use. To capture differences in land use, we coded each case and 1,000 y time period as HG = hunting and gathering land use only, Minimum Agg. = the presence of extensive agriculture; Moderate Agg. = the presence of extensive and intensive agricultural land use.

Once we integrated the KDE and ArchaeoGlobe data, we calculated the per capita growth rates of the mean KDE in each region as $\ln(MKDE_{t+1}/MKDE_t)$. We counted the number of consecutive generations with positive per capita growth in each case by the land use categories of HG, Minimum Agg., and Moderate Agg. If a given set of positive per capita growth rates crossed land use boundaries, we used the more productive land use category. For example, in the Northeast US region, one period of positive growth begins at 3,090 and ends at 2,820 cal BP. During this time period, extensive agricultural land use begins at 3,000 cal BP in the ArchaeoGlobe data. We recorded this period of growth as occurring in the Minimum Agg. category. Finally, we recorded the minimum and maximum per capita growth rate in each block of consecutive growth or decline (*SI Appendix*, Part III).

Data, Materials, and Software Availability. Raw and processed radiocarbon data and other stable isotope data have been deposited in NorthAmericaAdaptiveCap2 (https://doi.org/10.5281/zenodo.8217599) (61).

ACKNOWLEDGMENTS. We are grateful for financial support from the NSF, Grants: BCS-1535841 and IBSS-L:1520308. This study was also undertaken by J.F., E.R., and D.B. as part of PEOPLE 3000, a working group of the Past Global Changes (PAGES) project, which in turn received support from the Swiss Academy of Sciences and the Chinese Academy of Sciences. Finally, we would like to thank three anonymous reviewers and the editor for their helpful comments and suggested improvements on previous versions of the manuscript.

Author affiliations: [a]Anthropology Program, Utah State University, Logan, UT 84321; [b]The Ecology Center, Utah State University, Logan, UT 84321; [c]Native Environment Solutions LLC., Boise, ID 83701; [d]Division of Atmospheric Sciences, Desert Research Institute, Reno, NV 89512; [e]School of Human Evolution and Social Change, Arizona State University, Tempe, AZ 85281; [f]Department of Anthropology, Washington State University, Pullman, WA 99164; [g]University of Florida, Florida Museum of Natural History, Gainesville, FL 32611; [h]Department of Anthropology, University of Texas at San Antonio, San Antonio, TX 78249; [i]Department of Anthropology, The Center for Archaeological Research, University of Texas at San Antonio, San Antonio, TX 78249; and [j]School of Sustainabilty, Arizona State University, Tempe, AZ 85281

1. J.-P. Bocquet-Appel, O. Bar-Yosef, *The Neolithic Demographic Transition and Its Consequences* (Springer, 2008).
2. S. Shennan *et al.*, Regional population collapse followed initial agriculture booms in mid-Holocene Europe. *Nat. Commun.* **4**, 2486 (2013).
3. S. Shennan, "Population processes and their consequences in early Neolithic Central Europe" in *The Neolithic Demographic Transition and Its Consequences* (Springer, 2008), pp. 315–329.
4. S. Shennan, Demographic continuities and discontinuities in Neolithic Europe: Evidence, methods and implications. *J. Archaeol. Method Theory* **20**, 300–311 (2013).

5. E. R. Crema, Statistical inference of prehistoric demography from frequency distributions of radiocarbon dates: A review and a guide for the perplexed. *J. Archaeol. Method Theory* **29**, 1–32 (2022).
6. R. L. Kelly, T. A. Surovell, B. N. Shuman, G. M. Smith, A continuous climatic impact on Holocene human population in the Rocky Mountains. *Proc. Natl. Acad. Sci. U.S.A.* **110**, 443–447 (2013).
7. H. Jabran Zahid, E. Robinson, R. L. Kelly, Agriculture, population growth, and statistical analysis of the radiocarbon record. *Proc. Natl. Acad. Sci. U.S.A.* **113**, 931–935 (2016).
8. A. Bevan *et al*., Holocene fluctuations in human population demonstrate repeated links to food production and climate. *Proc. Natl. Acad. Sci. U.S.A.* **114**, E10524–E10531 (2017).
9. J. Freeman *et al*., Synchronization of energy consumption by human societies throughout the Holocene. *Proc. Natl. Acad. Sci. U.S.A.* **115**, 9962–9967 (2018).
10. D. Bird *et al*., A first empirical analysis of population stability in North America using radiocarbon records. *Holocene* **30**, 1345–1359 (2020).
11. J. Freeman *et al*., Landscape engineering impacts the long-term stability of agricultural populations. *Hum. Ecol.* **49**, 369–382 (2021).
12. A. Palmisano *et al*., Holocene landscape dynamics and long-term population trends in the Levant. *Holocene* **29**, 708–727 (2019).
13. P. V. Kirch *et al*., Reprint: Building and testing models of long-term agricultural intensification and population dynamics: A case study from the leeward Kohala Field system, Hawai'i. *Ecol. Model.* **241**, 54–64 (2012).
14. G. R. Milner, J. L. Boldsen, Population trends and the transition to agriculture: Global processes as seen from North America. *Proc. Natl. Acad. Sci. U.S.A.* **120**, e2209478119 (2023).
15. G. R. Milner, D. G. Anderson, M. T. Smith, "The distribution of Eastern Woodlands peoples at the prehistoric and historic interface" in *Societies in Eclipse: Archaeology of the Eastern Woodland Indians, A.D. 1400–1700*, D. S. Brose, C. Wesley Cowan, C. Robert Manifort, Jr., Eds. (Smithsonian Institution Press, Washington, DC, 2001), pp. 9–18.
16. G. R. Milner, *The Moundbuilders: Ancient Societies of Eastern North America* (Thames & Hudson, London, UK, ed. 1, 2004).
17. D. G. Anderson, Examining prehistoric settlement distribution in eastern North America. *Archaeol. East. N. Am.* **19**, 1–22 (1991).
18. D. Kondor *et al*., Explaining population booms and busts in mid-Holocene Europe. *Sci. Rep.* **13**, 9310 (2023).
19. E. A. Peralta *et al*., Past maize consumption correlates with population change in Central Western Argentina. *J. Anthropol. Archaeol.* **68**, 101457 (2022).
20. M. Lima *et al*., Ecology of the collapse of Rapa Nui Society. *Proc. R. Soc. B* **287**, 20200662 (2020).
21. M. Lima *et al*., Positive feedbacks in deep-time transitions of human populations. *Philos. Trans. R. Soc. B: Biol. Sci.* **379**, 20220256 (2024).
22. D. Bird *et al*., p3k14c, a synthetic global database of archaeological radiocarbon dates. *Sci. Data* **9**, 1–19 (2022).
23. J. E. Cohen, Population growth and earth's human carrying capacity. *Science* **269**, 341–346 (1995).
24. R. D. Lee, "Malthus and Boserup: A dynamic synthesis" in *The State of Population Theory: Forward from Malthus*, D. Coleman, R. Schofield, Eds. (Blackwell, Oxford, UK, 1986), pp. 96–130.
25. C. T. Lee, S. Tujapurkar, Population and prehistory. I: Food-dependent population growth in constant environments. *Theor. Popul. Biol.* **73**, 473–482 (2008).
26. C. T. Lee, C. O. Puleston, S. Tuljapurkar, Population and prehistory. III. Food-dependent demography in variable environments. *Theor. Popul. Biol.* **76**, 179–188 (2009).
27. C. O. Puleston, S. Tuljapurkar, Population and prehistory. II. Space-limited human populations in constant environments. *Theor. Popul. Biol.* **74**, 147–160 (2008).
28. C. Puleston, S. Tuljapurkar, B. Winterhalder, The invisible cliff: Abrupt imposition of Malthusian equilibrium in a natural-fertility, agrarian society. *PLoS ONE* **9**, e87541 (2014).
29. P. S. Meyer, J. H. Ausubel, Carrying capacity: A model with logistically varying limits. *Technol. Forecast. Soc. Change* **61**, 209–214 (1999).
30. J. W. Wood, A theory of preindustrial population dynamics: Demography, economy, and well-being in Malthusian systems. *Curr. Anthropol.* **39**, 99–135 (1998).
31. J. Wood, *The Biodemography of Subsistence Farming: Population, Food and Family* (Cambridge University Press, Cambridge, UK, 2020), vol. 87.
32. J. M. Anderies, Economic development, demographics, and renewable resources: A dynamical systems approach. *Environ. Dev. Econ.* **8**, 219–246 (2003).
33. J. M. Anderies, Culture and human agro-ecosystem dynamics: The Tsembaga of New Guinea. *J. Theor. Biol.* **192**, 515–530 (1998).
34. P. J. Richerson, R. Boyd, R. L. Bettinger, Cultural innovations and demographic change. *Hum. Biol.* **81**, 211–235 (2009).
35. P. J. Richerson, R. Boyd, Homage to Malthus, Ricardo, and Boserup toward a general theory of population, economic growth, environmental deterioration, wealth, and poverty. *Hum. Ecol. Rev.* **4**, 85–90 (1998).
36. J. Freeman, R. J. Hard, R. P. Mauldin, J. M. Anderies, Radiocarbon data may support a Malthus–Boserup model of hunter-gatherer population expansion. *J. Anthropol. Archaeol.* **63**, 101321 (2021).
37. V. I. Yukalov, E. P. Yukalova, D. Sornette, Punctuated evolution due to delayed carrying capacity. *Physica D* **238**, 1752–1767 (2009).
38. T. R. Malthus, *An Essay on the Principle of Population: Or, a View of Its Past and Present Effects on Human Happiness* (Reeves and Turner, London, UK, 1888).
39. E. Boserup, *Population and Technological Change? A Study of Long-Term Trends* (University of Chicago Press, Chicago, IL, 1981).
40. J. Freeman, R. P. Mauldin, M. Whisenhunt, R. J. Hard, J. M. Anderies, Repeated long-term population growth overshoots and recessions among hunter-gatherers. *Holocene* **33**, 1163–1175 (2023).
41. J. Freeman *et al*., The global ecology of human population density and interpreting changes in paleo-population density. *J. Archaeol. Sci.* **120**, 105168 (2020).
42. J. Freeman, The socioecology of territory size and a "work-around" hypothesis for the adoption of farming. *PLoS ONE* **11**, e0158743 (2016).
43. S. Shennan, R. Sear, Archaeology, demography and life history theory together can help us explain past and present population patterns. *Philos. Trans. R. Soc. B* **376**, 20190711 (2021).
44. G. R. Milner, *The Moundbuilders: Ancient Societies of Eastern North America* (Thames & Hudson, London, UK, ed. 2, 2004).
45. T. R. Pauketat, S. M. Alt, J. D. Kruchten, The emerald acropolis: Elevating the moon and water in the rise of Cahokia. *Antiquity* **91**, 207–222 (2017).
46. L. Stephens *et al*., Archaeological assessment reveals Earth's early transformation through land use. *Science* **365**, 897–902 (2019).
47. R. L. Kelly *et al*., A new radiocarbon database for the lower 48 states. *Am. Antiq.* **87**, 581–590 (2022).
48. E. C. Kansa *et al*., The Digital Index of North American Archaeology: Networking government data to navigate an uncertain future for the past. *Antiquity* **92**, 490–506 (2018).
49. J. J. Wells *et al*., Web-based discovery and integration of archaeological historic properties inventory data: The Digital Index of North American Archaeology (DINAA). *Lit. Linguist. Comput.* **29**, 349–360 (2014).
50. L. V. Benson, T. R. Pauketat, E. R. Cook, Cahokia's boom and bust in the context of climate change. *Am. Antiq.* **74**, 467–483 (2009).
51. B. W. Bird, J. J. Wilson, W. P. Gilhooly III, B. A. Steinman, L. Stamps, Midcontinental Native American population dynamics and late Holocene hydroclimate extremes. *Sci. Rep.* **7**, 41628 (2017).
52. C. R. Cobb *et al*., The beginning of the end: Abandonment micro-histories in the Mississippian vacant quarter. *J. Archaeol. Method Theory*, 1–25 (2023).
53. R. Gwinn Vivian, Chacoan roads: Function. *KIVA* **63**, 35–67 (1997).
54. L. Sebastian, *The Chaco Anasazi: Sociopolitical Evolution in the Prehistoric Southwest* (Cambridge University Press, 1996).
55. D. R. Abbott, A. M. Smith, E. Gallaga, Ballcourts and ceramics: The case for Hohokam marketplaces in the Arizona desert. *Am. Antiq.* **72**, 461–484 (2007).
56. S. R. Carpenter, W. A. Brock, E. H. van Carl Folke, Nes, and Marten Scheffer,, Allowing variance may enlarge the safe operating space for exploited ecosystems. *Proc. Natl. Acad. Sci. U.S.A.* **112**, 14384–14389 (2015).
57. N. N. Taleb, *Antifragile: Things that Gain from Disorder* (Random House Incorporated, 2012), vol. 3.
58. J. M. Anderies, A. A. Rodriguez, M. A. Janssen, O. Cifdaloz, Panaceas, uncertainty, and the robust control framework in sustainability science. *Proc. Natl. Acad. Sci. U.S.A.* **104**, 15194–15199 (2007).
59. L. B. Jorde, H. C. Harpending, Cross-spectral analysis of rainfall and human birth rate: An empirical test of a linear model. *J. Hum. Evol.* **5**, 129–138 (1976).
60. B. Ermentrout, Xppaut 5.96 (2006).
61. J. Freeman, Adaptive Capacity Tradeoff Data (2023) N.AmericaAdaptiveCap2. https://zenodo.org/records/10163554. Deposited 20 November 2023.
62. J. Freeman, R. Mauldin, R. J. Hard, people3k/Texas-Adaptive_Capacity: AdaptCapatTradeoff (1.0). Zenodo. https://doi.org/10.5281/zenodo.7757792 (Accesses 30 July 2023).
63. R. M. Tubbs, *Ethnic Identity and Diet in the Central Illinois River Valley* (Michigan State University, 2013).
64. S. H. Ambrose, J. Buikstra, H. W. Krueger, Status and gender differences in diet at Mound 72, Cahokia, revealed by isotopic analysis of bone. *J. Anthropol. Archaeol.* **22**, 217–226 (2003).
65. F. Rose, Intra-community variation in diet during the adoption of a new staple crop in the Eastern Woodlands. *Am. Antiq.* **73**, 413–439 (2008).
66. K. Hedman, E. A. Hargrave, S. H. Ambrose, Late Mississippian diet in the American Bottom: Stable isotope analyses of bone collagen and apatite. *Midcont. J. Archaeol.* **27**, 237–271 (2002).
67. B. Winterhalder, C. Goland, On population, foraging efficiency, and plant domestication. *Curr. Anthropol.* **34**, 710–715 (1993).
68. R. McAuliffe, R. P. Mauldin, S. L. Black, "Central Texas plant baking" in *Earth Ovens and Desert Lifeways: 10,000 Years of Indigenous Cooking in the Arid Landscapes of North America*, C. W. Koenig, M. R. Miller, Eds. (University of Utah Press, Salt lake City, UT, 2022), pp. 33–60.
69. R. P. Mauldin, D. L. Nickels, C. J. Broehm, Archaeological testing to determine the National Register eligibility status of 18 prehistoric sites on Camp Bowie, Brown County, Texas (Archaeological Survey Report, Center for Archaeological Research, The University of Texas at San Antonio, San Antonio, TX, 2003), vol. 334.
70. S. L. Black, D. G. Creel, "The Central Texas burned rock midden reconsidered" in *Hot Rock Cooking on the Greater Edwards Plateau: Four Burned Rock Midden Sites in West Central Texas, Studies in Archeology 22*, S. L. Black, L. W. Ellis, D. G. Creel, G. T. Goode, Eds. (Texas Archeaological Research Laboratory, The University of Texas at Austin, Austin, TX, 1997) , pp. 269–301.
71. E. R. Crema, A. Bevan, Inference from large sets of radiocarbon dates: Software and methods. *Radiocarbon* **63**, 23–39 (2021).
72. J. Freeman, D. A. Byers, E. Robinson, R. L. Kelly, Culture process and the interpretation of radiocarbon data. *Radiocarbon* **60**, 453–467 (2018).
73. E. R. Crema, A. Bevan, S. Shennan, Spatio-temporal approaches to archaeological radiocarbon dates. *J. Archaeol. Sci.* **87**, 1–9 (2017).
74. A. Timpson *et al*., Reconstructing regional population fluctuations in the European Neolithic using radiocarbon dates: A new case-study using an improved method. *J. Archaeol. Sci.* **52**, 549–557 (2014).
75. N. Williams Alan, The use of summed radiocarbon probability distributions in archaeology: A review of methods. *J. Archaeol. Sci.* **39**, 578–589 (2012).
76. T. A. Surovell, J. B. Finley, G. M. Smith, P. Jeffrey Brantingham, R. Kelly, Correcting temporal frequency distributions for taphonomic bias. *J. Archaeol. Sci.* **36**, 1715–1724 (2009).
77. L. E. Bluhm, T. A. Surovell, Validation of a global model of taphonomic bias using geologic radiocarbon ages. *Quatern. Res.* **91**, 325–328 (2019).
78. P. J. Reimer *et al*., The IntCal20 northern hemisphere radiocarbon age calibration curve (0–55 cal kbp). *Radiocarbon* **62**, 725–757 (2020).

Supporting Information for

The long-term expansion and recession of human populations

Jacob Freeman, Erick Robinson, Darcy Bird, Robert J. Hard, Raymond P. Mauldin, John M. Anderies

Corresponding Author: Jacob Freeman
E-mail: jacob.freeman@usu.edu

This PDF file includes:

Supporting Information Text

This document provides additional code and data analysis that supports the arguments made by Freeman et al. in "The long-term expansion and recession of human populations." In Part I, we provide the model code used to implement and numerically analyze the model presented in equations 1-3 of the main paper. We also provide additional analyses of the model's dynamics. In Part II, we first provide additional information on the collection and interpretation of data from the Central Texas and Middle Mississippi River Valley case studies. Second, we discuss edge effects and taphonomy in estimates of population from archaeological radiocarbon. In Part III, we provide additional analyses of the archaeological radiocarbon associated with ArchaeoGlobe regions.

Part I: Formal Model

In the main paper, we presented the results of three model experiments. These experiments were designed to answer the following questions. (1) How does adopting innovations that increase the productivity of a niche impact a region's population dynamics? (2) How does the interaction between increases in the productivity of a niche and the costs of social integration impact population stability in the presence of an innovation ceiling?

The model that we use can be distilled into the following equation: $growth = amplifying\ feedback - balancing\ feedback$. A key component of the model is that the balancing feedback may be weakened, endogenously, by fast changes in the production of food stimulated by population pressure. This creates a kind of treadmill or inertia effect. By this we mean that when innovations in food production are cheap and easy to implement, then a population can ratchet upward via a demographic transition. Such transitions occur in phases. At first, more people increases the *per capita* fitness of the population due to the amplifying feedback of population growth; however, eventually, competition for resources decreases the resources available per person, and *per capita* fitness declines with increases in population. Thus, a population needs to innovate again or enter an equilibrium where people can, on average, just replace themselves. Interestingly, if a population cannot effectively adopt innovations, then the history of past innovations has a large impact on whether a population will overshoot and then experience a painful recession or more smoothly transition into equilibrium. In particular, larger increases in the ability of a population to augment their resource base weakens the balancing feedback of competition for longer. Given the delays inherent in a population filling the space created by a production niche, this leads to larger overshoots and recessions.

Based on the model experiments presented in the main text, we can make the following generalization. Holding climate equal, in the presence of a delayed feedback from resources to human reproduction, any process that weakens the strength of the balancing feedback will generate expansion that occurs for too long followed by recessions. Fig. S1 illustrates the dynamics of *per capita* growth over time for the three experiments presented in the main text and helps illustrate the above generalization in a way that can be connected with data from real systems.

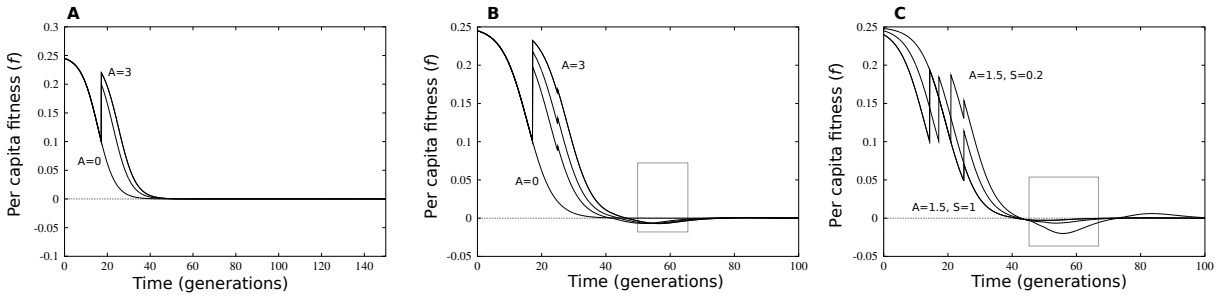

Fig. S1. A: Graph of demographic transitions overtime that corresponds with Fig. 1A and B in the main text: $S = 0.5$, $d = 0$, $C = 1$, $r = 0.25$. As A increases, the productivity of resources increases and the length of demographic transition increases. B: Graph of demographic transitions over time corresponding to Fig. 1C and D in the main text: $S = 0.5$, $d = 25$, $C = 1$, $r = 0.25$. The delayed impact of human populations on the resource stock results in *per capita* growth rates turning negative (grey box) during a population recession. C: Demographic transitions over time corresponding to Fig. 1E and F in the main text. In each successive curve we hold $C = 1$, $d = 25$, $r = 0.25$, and $A = 1.5$. We vary the cost of social integration. As S increases, the length of the demographic transition increases and recessions become more severe (grey box).

Fig. S1A illustrates that as the ability to augment the productivity of resources increases ($A_2 - A_1$ increases), the length of the demographic transition increases. This is to say that once the minimum fitness of 0.1 is reached, this triggers a shift toward a more productive resource niche. The larger the increase in $A_2 - A_1$, the longer it takes *per capita* growth to return to the population pressure fitness level of 0.1. This same pattern is displayed in Figs. S1 B and C. These Figs. replicate the experiments presented in Fig. 1C-F in the main paper. The main difference now is that human populations have a delayed impact on their resource base. As above, larger increases in the ability to augment the productivity of resources increases the length of a demographic transition. Further, increases in the ability to augment the productivity of resources also results in a larger population recession. This is noted Figs. S1 B and C by the grey rectangles. These grey rectangles mark the time period where *per capita* fitness turns negative.

The effect of intrinsic growth rate, r on long-term population dynamics. As defined in the main text, r (1/time) is the per capita rate of population growth in the absence of environmental or social constraints (i.e., the "intrinsic" growth rate) and is a

basic parameter of the logistic model. Here, we discuss the effects of changes in r on the population dynamics of the system. Holding all other parameters equal, the ratio of the intrinsic growth rate, r to the relationship between the productivity of resources and population density, B_i controls whether the system displays long-term oscillations or smoothly transitions into equilibrium. For example, in Fig. S2A, we hold the increase in productivity from an innovation equal ($A = 2$, S =0.5, C=1, $B_1 = 0$, B_2=-0.25), and allow for a delay. Recall here that B_2 defines the relationship population density and the productivity of resources once an innovation has occurred and moved the system from $K_1(t)$ to $K_2(t)$ resource constraints. At very low-levels of r the system displays a smooth transition to equilibrium when it hits an innovation ceiling. Increase r and low values of B_2 lead to overshoots and recessions. Note that in Fig. S2A the humped shape of the curve becomes more dramatic as r increases, and the population recesses into equilibrium.

Fig. S2B holds $A = 2$, S =0.5, C=1, $B_1 = 0$, and r=0.05. In this set of numerical experiments, intrinsic population growth is much more constrained. As a consequence, it takes a more negative relationship between population density and human impacts on ecosystem productivity to generate oscillations. As B_2 becomes more negative, we observe a larger recession, and we observe repeated oscillations. This occurs because, as in classic human-resource models such as Anderies' model of Tsembaga agriculture (1), there is a delay between impacts on resources and population density. At more negative values of B_2, resource depression leads to a drop in population density, but resources begin to recover as human population density goes down. Due to the delay in human impacts on resources, population begins to grow again until growth outpaces resource recovery, and the population declines again.

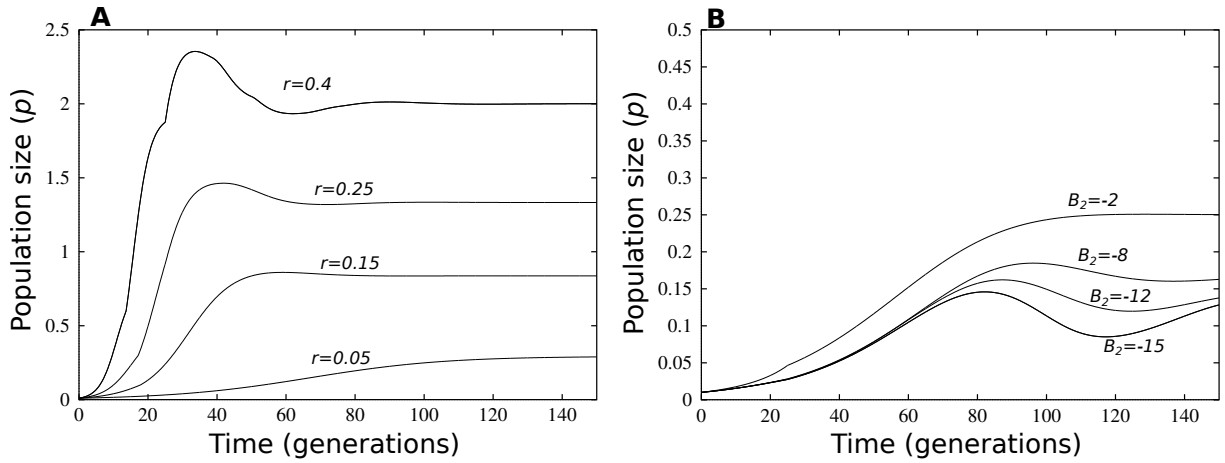

Fig. S2. A: Population dynamics over time for different values of r holding S=0.5, d=25, C=1, A=2, B_1=0 and B_2=-0.25. B: Population dynamics over time for different values of B_2 holding S=0.5, d=25, C=1, A=2, B_1=0, and r=0.05.

In sum, as noted in the main paper, when innovations increase productivity and lower the costs of social integration, then overshoots and recessions are generated. Holding all else equal, the severity of such damped oscillations is impacted by the ratio r to B_2. Very low-levels of r simply mean that a more negative B_2 is necessary to generate recessions. This suggests the hypothesis that in cases where we observe similar levels of social integration and increases in productivity over time but only observe overshoots and recessions in some cases, it could be due to the fact that human impacts on resources are not as severe in those cases. It is also possible that innovations, in addition to increasing A, could also increase r. That is, better technology leads to a higher intrinsic (unconstrained) rate of reproduction. If this is the case, then the increase in r could also contribute to overshoots and recessions near an innovation ceiling. This does not change our hypotheses in the main text.

Model Code. Below is the code for analyzing the model in XPPAUT. We analyzed the model numerically over 200 time steps.

```
# delayed feedback in a population growth model: delayFinal.ode

# declare all the parameters, initializing the delay to 0
p tau=0,B1=0,r=0.25,coop=0, comp=1, alpha=2, tau2=0, B2=0, resp=0,
rmean=1,rsigma=0, Amin=0.5, fitmin=0.1, A=.25


##Hidden functions

###define scale of social integration due to more inclusive institutions.
Set comp=1, 0>=coop<1

S=comp-coop
```

```
#Add stochastic process for ecosystem productivity with mean and standard
#deviation. In the model we analyze, w is set to 0.
#Thus, no stochastic variation in pro.

wiener w
pro = max(rmean*(1 + rsigma*w),Amin)

#niche capacity is the balance of positive and negative effects on the
#productivity of #ecosystems due to human activity. These impacts can have
#different delays from 0 to 35 #generations

##Strategy one niche capacity
cap=B1*delay(p,tau2)

##Strategy two niche capacity
cap2=B2*delay(p,tau2)


#Define the change in ecosystem capacity to support humans as climate driven
#productivity plus #niche construction capacity

#####First, we write the fitness fuction. Note the delay defined as tau here. We do
#not study this delay here, and thus set tau =0.
#However, it is included because the ability
#to detect population pressure through competitive signals
#and respond to such signals is another potential
#delay point or, rather, process that may take time.

fit1=r-(S/Kt)*delay(p,tau)

########Next we defin kt as climate driven productivity
#plus the niche capacity of strategy one.
Kt=pro+cap

###We define kt2 as climate driven productivity plus
#the niche capacity of strategy two.
Kt2=pro+A+cap2

##I is an if then fucntion. If fit1<fitmin,
#then there is population pressure, and the mean
#agent switches to Kt2
I= if (fit1<fitmin) then (Kt2) else (Kt)


# population growth equation
p'= (r*p)-((S*p^alpha)/I)

##Set initial condition of p
init p=.01


# set maxdelay
@ delay=35

aux niche=cap
aux Car=Kt
aux pp=p/Kt
aux fit=r-((S/I)*p)
aux It=I

@ total=150, xlo=0,xhi=150,ylo=0,yhi=2.5
```

```
# done
d
```

Part II: The Middle Mississippi and Central Texas Case Studies

The foundation of our analysis is a controlled comparison of the Middle Mississippi River Valley and Central Texas. As noted in the main paper, these regions have similar ecosystems (grassland to wooded savanna), abundant evidence of changes in resource extraction over the last 3,500 years, and significant differences in social-ecological adaptations. People in the Middle Mississippi River Valley adopted agriculture and, eventually, large centers of population aggregation (e.g., Cahokia). The people of Central Texas intensified their production of wild resources, especially wild roots and bulbs over the last 3,500 years, and remained mobile hunter-gatherers. To begin evaluating the Adaptive Capacity Tradeoff model, we needed to construct estimates of changes in resource extraction over time. In particular, we needed to develop indicators of the consumption of energy dense carbohydrate resources that might fuel waves of demographic transitions and, thus, net population growth over thousands of years. In order to develop estimates of changes in resource extraction, we used two classes of data: Human bone isotopes and a production index of carbohydrate use.

Human Bone Isotopes. We conducted a literature search to collect previously published data on human bone isotopes from each of our case study regions. Recent compilations of these data were available in Central Texas made by Freeman and colleagues (2), and we built a database specifically for this study for the Middle Mississippi River Valley. Fig. S3 illustrates the locations of the archaeological sites used to construct the human bone isotope data sets, and the data are openly available as part of this publication.

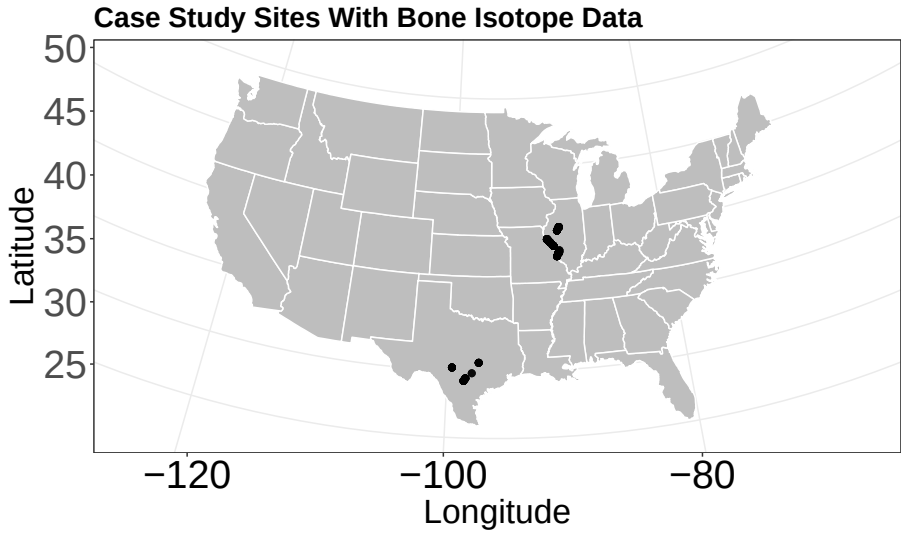

Fig. S3. Map of sites from which samples of human bone were analysed and reported on in the literature consulted as part of our study.

The use of stable isotopes has a long history in archaeology. Much current research tackles the problem of reconstructing the diet of individuals over their life history or dealing with potential issues related to multiple diets resulting in similar stable isotope signatures in human tissues. Here, we are not concerned with reconstructing specific diets. Rather, we are interested in detecting shifts in protein and carbohydrate consumption. To this end, we use two basic patterns to help interpret $\delta^{15}N$ (and $\delta^{13}C$) isotopes in human bone over time in both case study regions.

(1) In terrestrial environments, plant stable carbon isotopic abundances, expressed as parts per thousand (‰), broadly reflect the use of one of three photosynthetic pathways (C_3, C_4, and CAM) by plants to incorporate atmospheric carbon into their tissue (3–5). The C_3 pathway discriminates against the heavier stable isotope of carbon (^{13}C) relative to the lighter isotope (^{12}C), resulting in lower $\delta^{13}C$ values in C_3 plants. Most plants, including all trees and nuts, cool season grasses, most bushes, shrubs, and flowers, and geophytes, use the C_3 pathway (6–8). At a global level, values for C_3 plants typically range between -37 and -20 ‰, with an average of -26.5 ‰ (9–12). Terrestrial plants that use the C_4 pathway, which evolved in hot, arid settings are much less common than C_3 plants. Composed primarily of warm season grasses, the C_4 pathway does not discriminate against the heavier ^{13}C isotope to the degree seen in C_3 plants, resulting in values closer to that of atmospheric

carbon, which has a modern $\delta^{13}C$ value of -8 ‰ (13). The $\delta^{13}C$ isotopic values of C_4 plants fall between -16 and -9 ‰, with a global average of about -12.5 ‰ (10–12). The third pathway, CAM, is present in cacti and most other desert succulents. The carbon isotopic values of CAM plants have a wide range (see 12, 14–16), though in arid and semi-arid settings, they tend to mimic the isotopic range of C_4 plants (17).

(2) Variation in nitrogen ($\delta^{15}N$) stable isotope values stems in part from trophic level enrichment within a food web (18–20). Atmospheric nitrogen (N_2, $\delta^{15}N = 0$ ‰) is absorbed by plants either through the soil or, for legumes, through the air (21). Plant $\delta^{15}N$ typically ranges between 1 to 6 ‰, with non-leguminous plants tending to dominate the higher end of that range (22, 23). The $\delta^{15}N$ in herbivores feeding on plants is enriched above the values of the consumed plants, and carnivores have $\delta^{15}N$ values higher than herbivores. The degree of $\delta^{15}N$ enrichment in bone varies, but is estimated between 3 and 4 ‰ for each trophic level. As many aquatic food webs are complex ecosystems relative to terrestrial settings, the increase in $\delta^{15}N$ is especially apparent (see 24–28).

As humans consume resources, the $\delta^{13}C$ and $\delta^{15}N$ isotopic signatures present in those resources incorporate into flesh, organs, and bone, though with additional shifts depending on the tissue (29–31). While the relationship is complex in omnivores (32, 33), carbon routed to the organic component of bone (collagen) generally has values +5 ‰ higher than consumed plant values. Carbon routed to the mineral component of bone (apatite) increases by around +10 to +12 ‰ relative to the plant signature (11, 20, 34, 35). Collagen contains both carbon and nitrogen isotopic signatures, and the nitrogen and carbon in collagen primarily reflects protein consumption (3, 31, 36–38). While certainly present, plants tend to have low quantities of nitrogen. Protein in bone collagen primarily derives from animal consumption. Several researchers illustrate that in omnivores a linear relationship exists between $\delta^{13}C$ carbon values in collagen and diet, but only within a C_3 or a C_4/CAM protein group (32, 33). In contrast, $\delta^{13}C$ carbon values in bone apatite correlates with the isotopic signature of the whole diet (32, 33). Isotopic studies of carbon in collagen and apatite complement each other and, ideally, when coupled with nitrogen signatures in collagen, may provide data to reconstruct past diets.

Of course reconstructing past diets also requires a knowledge of the resources in local ecosystems and the isotopic signatures of these resources. Here, as noted, we are not concerned with reconstructing the specific diets but, rather with detecting shifts in protein consumption. Thus, we focus our analysis on $\delta^{15}N$ and whether these values decline as human population densities increase in a region as people potentially shift consumption away from fish and land animals and toward more carbohydrate dense plants. In general, the Middle Mississippi River Valley has larger river systems than Central Texas and more evidence of fishing and aquatic resource use. Thus, we would expect that, overall, $\delta^{15}N$ would be higher in the Middle Mississippi than Central Texas. This is indeed the case, with a median $\delta^{15}N$ value of 9.9‰ in the Middle Mississippi and a median value of 8.94‰ in Central Texas. Yet, given these differences in overall $\delta^{15}N$ values, we still see the same pattern over time: A slight increase in $\delta^{15}N$ values as the population increases rapidly and then a significant decline in $\delta^{15}N$ near peak population density (Fig. 3 in the main text). Of course, it would be an assumption to conclude from this evidence *alone* that declines in $\delta^{15}N$ result from shifts in diet toward more carbohydrates. Thus, we used indexes of carbohydrate production to further evaluate this assumption.

Mississippi River Valley Carbohydrate Index. In the Middle Mississippi River Valley, we used a cultivation index developed by (39) to track changes in the production of domesticated seeds rich in carbohydrates but that require higher processing times and, often, have lower protein. Milner and Boldsen's cultivation index was developed at the site level from much of eastern North America; however, a core of sites come from Illinois and just across the border in Missouri. These sites overlap with the core of the Middle Mississippi River valley case study, as defined here.

The use of domesticates in the Middle Mississippi River and much of Eastern North America is complex, though certainly not unique. The initial adoption of domesticates included multiple native plant species, such as species of amaranth and chenopodium. These are C_3 plants domesticated prior to the study period, which begins at 3,500 cal BP. Later, in the American Bottom (core of the Middle Mississippi case study) maize was adopted abruptly around 1050 cal BP (40). Maize has a C_4 photosynthetic pathway, and increased consumption enriches $\delta^{13}C$ isotope values, as discussed above. Thus, we can infer when intensive maize use began, but we are concerned here with the use of cultigens more broadly, not maize specifically. Milner and Boldsen constructed their cultigen index by recording "Eastern Agricultural Complex (EAC) plants [that] included goosefoot (*Chenopodium berlandieri*), erect knotweed (*Polygonum erectum*), maygrass (*Phalaris caroliniana*), marshelder (*Iva annua*), little barley (*Hordeum pusillum*), sunflower (*Helianthus annuus*), and cucurbits (members of the *Cucurbitaceae*)" (41), and Introduced plants (IP), including maize (*Zea mays*) and beans (*Phaseolus vulgaris*) (41). They recorded the frequency of these cultigens in flotation samples as well as the frequency of nuts. As stated by Milner and Boldsen:

> "The intent is not to estimate the proportions of various plants in diets. That is impossible with the kinds of material archaeologically recovered. Instead the plant remains indicate when the contributions of various kinds of food – those classified here as wild, EAC, and IP – changed relative to one another. More precisely, they track change in terms of the charred material that happened to be preserved, recovered from archaeological sites, and listed in (normally detailed) reports (41)"

The assumption, as noted in the main text, is that the more cultigens relative to nuts, the more that people were processing high carbohydrate, but lower protein resources relative to wild plants (nuts). Thus, higher frequencies were preserved in archaeological sites.

Fig. S4 displays the relationship between $\delta^{13}C$ collagen and the cultivation index over time in the Middle Mississippi River Valley. Consistent with the arguments made in the main paper, the cultivation index increases through time, with a significant

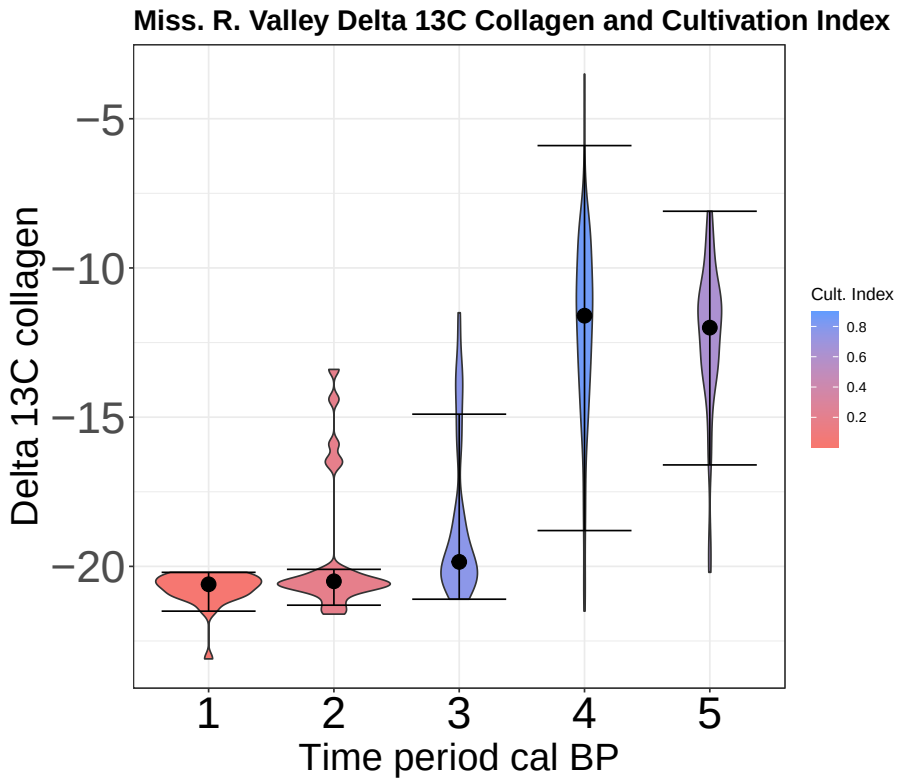

Fig. S4. Violin plots of $\delta^{13}C$ from 354 individuals in the Middle Mississippi River. Each violin plot is shaded by the median cultigen index during cultural historical time periods. Black dots indicate the median of the distribution and error bars 95 % of the distribution.

increase from period 2 (Early Late Woodland) to period 3 (Late Late Woodland). This uptick in cultigens corresponds with a significant decline in $\delta^{15}N$, as noted in the main paper. Interestingly, and consistent with the arguments of Emerson and colleagues (40), we observe a significant increase in $\delta^{13}C$ collagen from period 3 to period 4 (the Mississippian) but no significant increase in the cultigen index. In effect, maize replaces, though not completely, the Eastern Agricultural Complex, and maize remains dominant even during period 5 as population declined and $\delta^{15}N$ increased. Of course this last increase in $\delta^{15}N$ only reflects one large site, so it should be interpreted with some caution.

Fig. S5 displays box plots of the cultigen index by cultural historical periods for the core sites from Illinois and Missouri that occur in close proximity to sites from which human bone isotope data are recorded. Using a Mann-Whitney U test, there is a significant increase in the cultigen index from period 1 to period 2 (W = 554, p-value = 0.0005858) and from period 2 to period 3 (W = 544, p-value = 1.167e-06). There is not a statistically significant difference between periods 3 and 4. There is a significant difference between periods 4 and 5 (W = 461, p-value = 0.05572). The important point here is that the differences in the median value of the cultigen index that we document in the main paper are large and significant in the statistical sense. The roughly 47 generations of positive *per capita* population growth (i.e., increasing well-being) from 2240 cal BP to 830 cal BP was fueled by incremental increases in the production of carbohydrates until about 1000 cal BP. At that point, the ratchet could, it seems, no longer turn as the system approached an innovation ceiling, in terms of food production.

Fig. S6 compares the cultivation index of sites included as part of the core case study area and sites excluded from the analysis. Among the excluded sites, the overall pattern remains of increasing use of cultigens through time, however there is a lot more variability. The higher variability is not surprising since the sample from the mid continent covers a very large geographic area. If we add the excluded sites to the included sites and conduct the analysis, we still observe a significant increase in the cultigen index from period 1 to period 2 (W = 1118.5, p-value = 0.0001671) and from period 2 to period 3 (W = 895, p-value = 5.349e-07). There is not a statistically significant difference between periods 3 and 4. There is a significant difference between periods 4 and 5 (W = 1725, p-value = 0.09078). A cautious way to interpret this pattern is that the strength of the trend of increasing cultigens and then a final decline in cultigens among the included sites from Illinois and Missouri "overpowers" the increased variability documented among sites excluded from our main analysis. This is not surprising since the included sites (160) comprise a little more than half the sample (304 total sites).

Central Texas Carbohydrate Index. To estimate the intensity of carbohydrate production in Central Texas, we use an index of large to small burned rock features that likely resulted from earth oven cooking. The features included in our data set range in size from small hearths roughly a meter or less in diameter to accumulations of shattered rock often forming circular mounds one meter high and over 10 meters across. These larger features, often termed burned rock middens (BRMs), represented

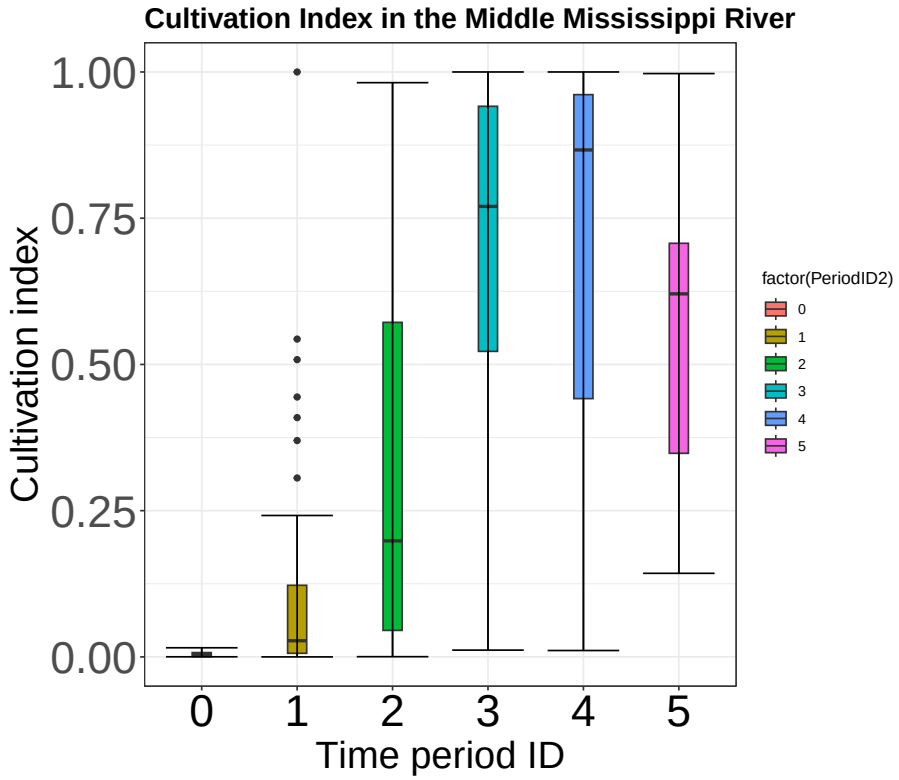

Fig. S5. Box and whisker plot of the cultivation index values by cultural historical time period for included sites in the Middle Mississippi River Valley case study.

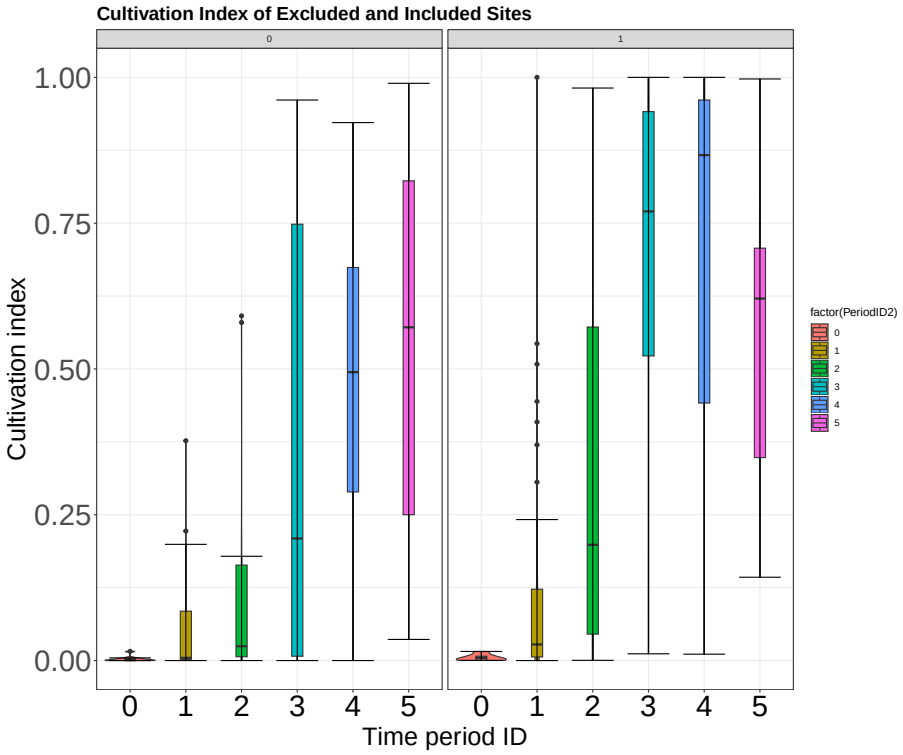

Fig. S6. Box and whisker plots of the cultivation index values by excluded sites from our study (panel 0), included sites (panel 1), and cultural historical time period from the mid-continent of Eastern North America.

larger and more repeated cooking events, potentially hundreds of uses (42–44). To understand the logic of this index, it is

important to consider the technology of earth ovens, what they were used for in Central Texas, and hunter-gatherer land use.

Although earth ovens are a general cooking technology, evidence in Central Texas suggests that they were often, if not primarily, used to bake plants rich in carbohydrates (e.g., 45–50). This inference comes from two lines of evidence. (1) Ethnographic descriptions and experimental research suggest that a pit was excavated and lined with rock. A fire was then built and allowed to die down. Food, often wrapped in moist, green vegetation, was subsequently placed on the heated rock and coals in the center of the oven, and the pit sealed with earth. The stored heat in the rock dissipated over several hours or days, baking the feature contents. When the food was cooked, the feature was opened and the contents removed. Repeated heating and cooling of the rocks in the pit results in breakage and such broken rocks become discarded, along with charcoal and ash, usually around the central pit (e.g., 51–56). (2) In the Central Texas region, hundreds of burned bulb fragments recovered from feature macrobotanical and flotation samples indicate that these features were used to roast geophytes, such as: Wild onion (*Allium sp.*), Eastern camas (*Camassia scilloides*), and dog's-tooth violet (*Erythronium mesochoreum*) (e.g., 57–60).

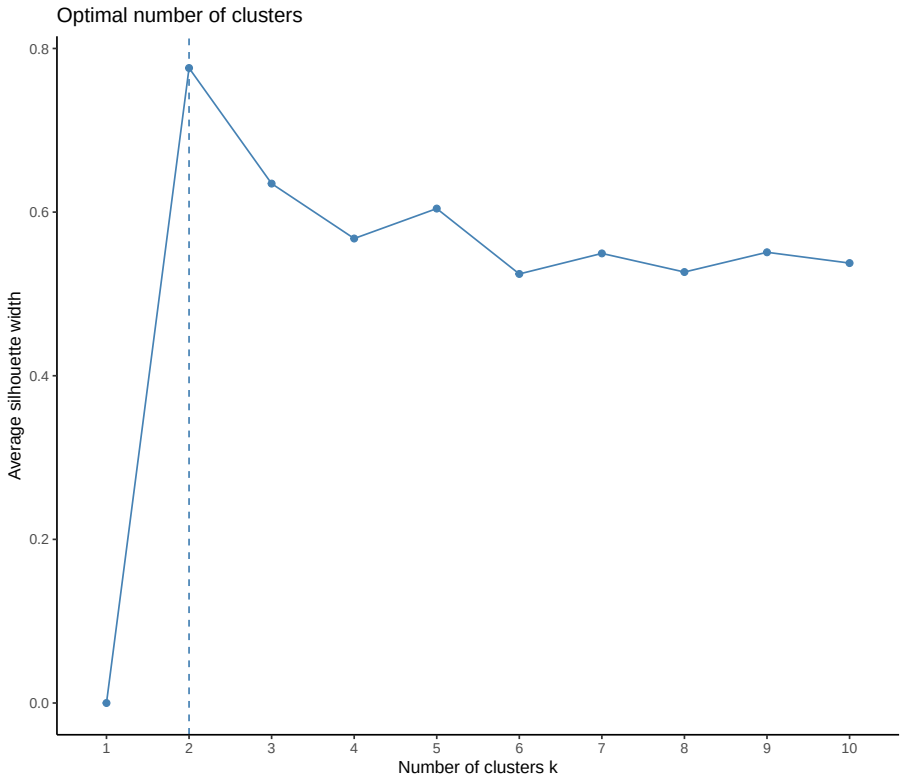

Fig. S7. Silhouette plot for a K-medoids cluster analysis. The plot suggests that two clusters is the optimal solution. That is, there are two distinct groups of burned rock features in the data set.

Land use is the key to understanding how large burned rock middens form and become more frequent on a landscape. Such middens form when large earth ovens are used repeatedly over time. Large burned rock middens may form in a couple of ways. (1) Certain land forms, like the entrance of a rock shelter, constrains the space available for cooking. If people revisit these locations over hundreds to thousands of years, large middens will form simply because space to dig a cooking pit is limited and people will use the same location over and over again, resulting in many discarded rocks, ash, etc. accumulating over time. (2) In open air sites, like the majority of sites in Central Texas, the land use system must be organized in such a way that people visit the same locations over and over again, baking geophytes from nearby patches. In large scale systems less focused on carbohydrate production, foragers should rotate their territories over time, and we should expect earth oven use to result in many smaller burned rock features. For example, imagine a 100 square km landscape that foragers use with patches of geophytes evenly dispersed over the territory. If a forager group rotates their territory in 10 square kilometer sections every decade or so, then this group will use many different geophyte patches a few times, resulting in a high frequency of smaller features. Now imagine that a group only uses a 10 square kilometer section, never rotating territories. Such a strategy will result in the best geophyte locations being used over and over again. It will also necessitate that the group consume more of such resources because they have much less territory to search for animals. Thus, as land use shifts toward smaller territories and more consumption of carbohydrates, we should expect the repeated use of earth oven locations to increase dramatically and the large features to become much more frequent on the landscape relative to small features.

To build the burned rock midden index, we collected radiocarbon dated features from published sources, including earlier compilations (44, 49, 57, 58, 61–64), and we calculated the surface area of each feature (see (2)). These are important classes of data because a greater frequency of such features and surface area are both estimates of more investment in baking resources

that require prolonged heat exposure to unlock carbohydrates for consumption. Ethnographic and experimental evidence indicates that fire-cracked rock is a byproduct of repeated heating events, in this case, baking events (49, 53, 63). Surface area serves as a estimate for the number of fire-cracked rocks (Spearman's ρ=0.86) and weight of rocks contained in a feature (Spearman's ρ=0.75). More fire-cracked rock indicates greater investment in carbohydrate rich resource extraction (49, 53).

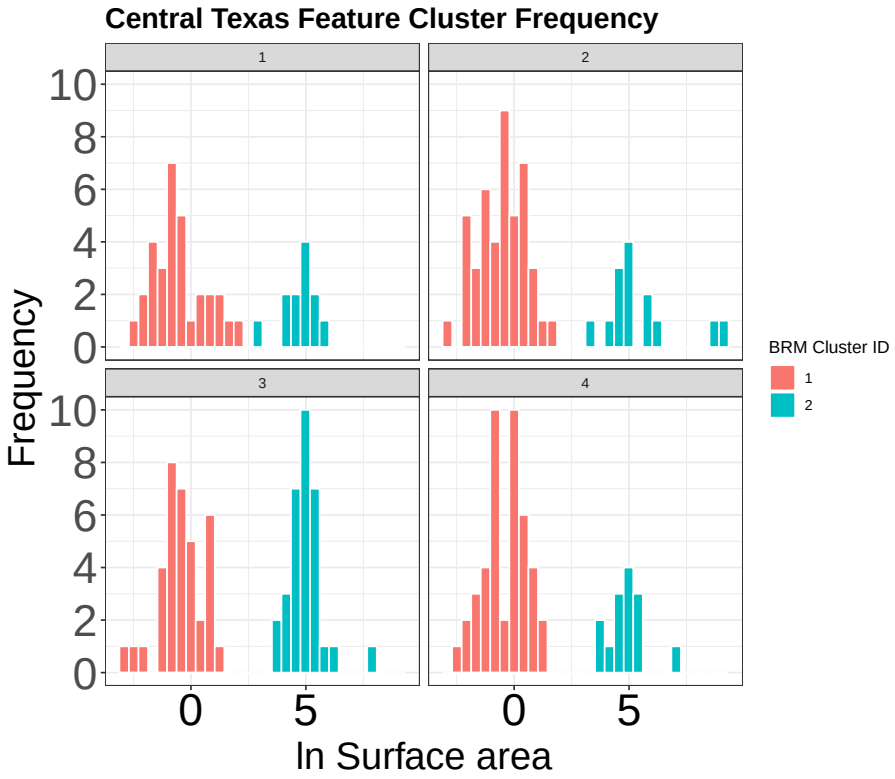

Fig. S8. The frequency of small and large fire cracked rock features over time in Central Texas. Panel 1=Early Late Archaic (3,699 to 2,000 cal BP); 2= Terminal Late Archaic (1,999 to 1,300 Cal BP);3= Late Prehistoric I (1,299 to 650 cal BP); and 4= Late Prehistoric II (650 to 400 cal BP).

To construct a time-series of changes in feature surface area, we collected data on 301 burned rock features, including radiocarbon ages from organic materials directly associated with these features. We used rcarbon (65) to calculate the median age of each radiocarbon age associated with a burned rock feature. Where features had more than one radiocarbon age, we averaged these ages. Next, we calculated the mean surface area of all features by traditional cultural historical time-periods in Central Texas. We broke some of the larger intervals into early and late. The intervals include, Early Late Archaic (3,699 to 2,000 cal BP), Terminal Late Archaic (1,999 to 1,300 Cal BP), Late Prehistoric I (1,299 to 650 cal BP), Late Prehistoric II (650 to 400 cal BP).

We then ran a k-medoids cluster analysis on all of the dated features, clustering on the natural log of surface area. Fig. S7 illustrates that the optimal cluster solution is 2 groups. Or, rather, the cluster analysis lends support to our visual identification of a bimodal distribution of feature surface areas in the data. Fig. S8 illustrates the distinct clusters of burned rock features and the change in the frequency of these features over time. Note the two distinct distributions of feature surface area. Cluster 1 has a modal area of ln=0, or 1 square meter, and cluster 2 has a modal surface area of about ln=4.5 or a little over 90 square meters. Large burned rock features first emerge between 4,200 and 3,500 cal BP (2). After this time period, Fig. S8 illustrates how during period one, the frequency of small features is higher than large features. However, large features become more prevalent relative to small features during period 2 and more prevalent overall than small features during period 3. As noted in the main text, large features then decline in frequency during period 4 relative to small features.

In addition to the significant declines in nitrogen isotopes documented during period 3 in the main paper, Freeman and colleagues (2, Fig. 3) also demonstrate a significant decline in $\delta^{13}C$ collagen and carbonate values. Geophytes are C_3 plants, and, thus, this decline in $\delta^{13}C$ is consistent with an increased consumption of carbohydrates from geophytes produced in large earth oven features.

Mississippi River Valley and Central Texas Population Dynamics. We used two methods to reconstruct the past population dynamics of the two case studies. The method used in our main analysis was to construct a mean kernel density estimate from 200 kernel density estimate simulations. These simulations were run in rcarbon using a bandwidth of 50 and an h function of 100 to smooth the KDEs (65). This method emphasizes the long-term trend of the frequency of calibrated radiocarbon ages and smooths variation. In a sense, it is type 1 error conservative, minimizing fluctuations that may result from the

calibration process itself or sample biases (i.e., minimizing the detection of false short-term fluctuations). Of course, minimizing fluctuations also means potentially missing or ignoring short-term fluctuations in archaeological radiocarbon frequency that actually result from changes in the occupation intensity of an area (type 2 error).

In addition to the mean KDE approach, we also constructed SPDs in rcarbon using a 100 year smoothing function and an h-function of 100 (65). We then fit a logistic model to the SPDs and used the 'modelTest' function to generate random calendar year dates via Monte-Carlo simulation (n=100) and back-calibrated into ^{14}C ages to generate a null 95 % confidence envelope for each logistic model (65). In both cases, the global fit of the logistic model is statistically significant at $p < 0.05$. This null model approach provides a different perspective, capturing both the trend of the data over time and allowing one to assess deviations from the trend. Fig. S9 illustrates the results of this analysis.

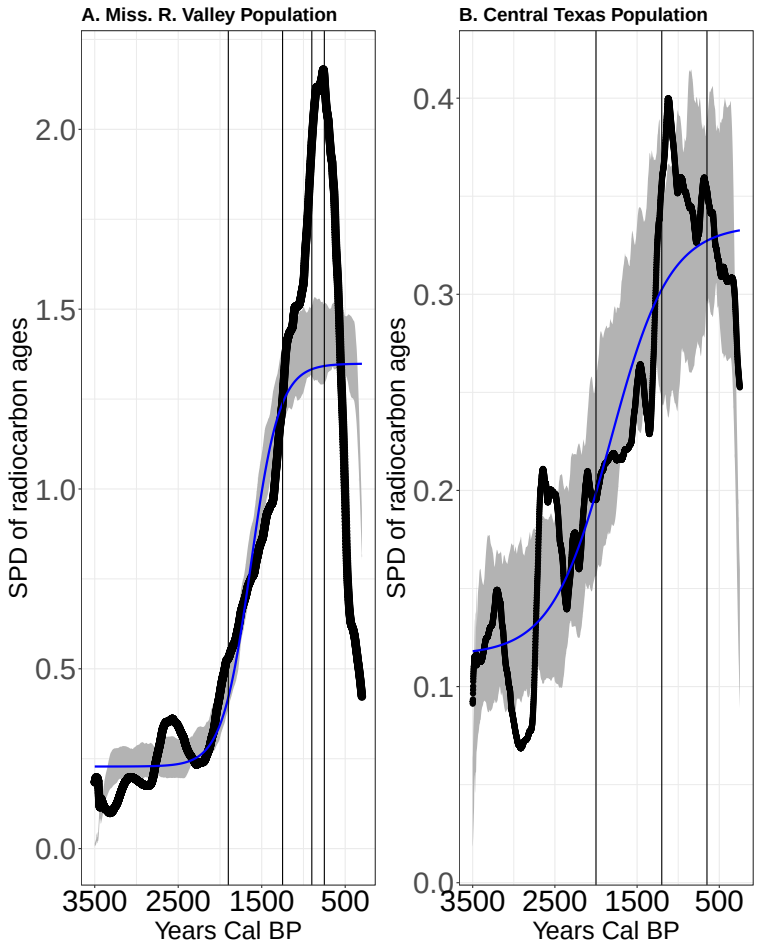

Fig. S9. A-SPD and 95 % confidence envelope for a logistic null model in the Middle Mississippi River Valley. B-SPD and 95 % confidence envelope for a logistic null model in Central Texas. Vertical reference lines indicate the cultural historical periods discussed in the main text

Fig. S9 replicates the mean KDE analysis presented in the main paper. At first, in both regions, population increases slowly. Population then increases much more rapidly between 2,500 and 800 cal BP. From 1,400 to 800 cal BP in the middle Mississippi River Basin, there is a large overshoot of the null logistic model and a smaller overshoot of the logistic null model occurs around 1,000-800 cal BP in Central Texas. Similarly, following this overshoot, the recession of carrying capacity is much more intense in the Middle Mississippi than in Central Texas.

Fig. S10 illustrates the *per capita* growth rates of the SPDs displayed above (summed into 30 year generations). Note that the *per capita* growth rates are more variable than those calculated from the mean KDEs in the main paper (i.e., the SPDs are more sensitive to type 1 than type 2 error). However, the same patterns are still apparent. There is a roughly 47 generation long time period from 2,200 to 830 cal BP in which the Middle Mississippi River valley experienced positive *per capita* growth. This means that the mean fitness or well-being increases for almost 50 consecutive generations! Conversely, Central Texas displays shorter periods of positive *per capita* growth interspersed by short periods of negative growth. The exponential-like increase of population over 3,000 years, thus, was achieved differently in these two case studies.

As noted in the main text, the patterns of growth and resource extraction in these regions are consistent with the Adaptive Capacity Tradeoff. However, there is one clear pattern that does not fit the model. Our model, like those of previous researchers (e.g., 66–69), encodes the Boserupian idea that population pressure drives innovations. Specifically, there is a minimum tolerable

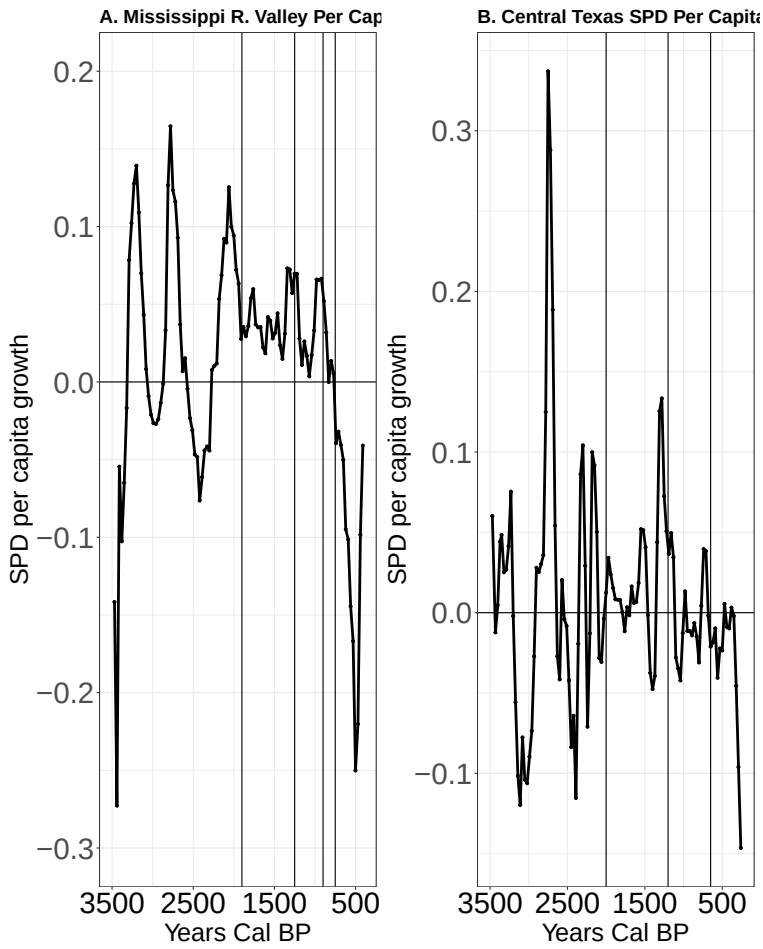

Fig. S10. A-*Per capita* growth of the 100 year smoothed SPD summed into 30 year generations in the Middle Mississippi River Valley. B-*Per capita* growth of the 100 year smoothed SPD summed into 30 year generations in Central Texas. Vertical reference lines indicate the cultural historical periods discussed in the main text

well-being greater than demographic replacement (i.e., *per capita* growth =0) that, once crossed, motivates the adoption of innovations in the production of food. This assumption suggests that *per capita* growth remains positive for dozens of generations as populations continually ratchet up their production of food until they hit an innovation ceiling. We observe this pattern in the Middle Mississippi River Valley. Yet, in Central Texas, *per capita* growth rates often turn negative. It appears that rather than getting stuck in a demographic equilibrium, this hunter-gatherer system continually increased the production of carbohydrates even though mean fitness declined for a few generations at a time. It was like two steps forward, one step back. This suggests that innovations can be adopted even during periods in which population pressure is so high that the mean fitness of a population is declining! This pattern is a real surprise in light of the often cited idea that extreme population pressure should limit innovations (70). It may be that hunter-gatherer systems spend more time near the limits of their infrastructure systems and, thus, display more instability overall due to delayed impacts on resources. More work is needed to understand the generality of these patterns.

Edge effects and taphonomy. As mentioned in the main text, archaeologists worry that the shapes of the KDE and SPDs above might be impacted by two processes: Edge effects and taphonomy. A key underlying assumption of the approach used in this paper is that large samples of radiocarbon ages collected by archaeologists reflects the underlying growth of human populations and economies in a given area (71, 72). The larger the economy and number of people, the more organic waste remains become traces of past human activity and potentially observed in archaeological contexts (73, 74). Though multiple studies document a link between multiple estimates of population and large samples of radiocarbon (e.g., 71, 75–77), edge effects and taphonomy could still possibly impact the link between past population and the sampling of archaeological radiocarbon. We consider these issues and their relevance to our analysis below.

Edge effects. An "edge effect" results when archaeologists do not randomly sample radiocarbon ages across time periods. Rather, because of the presence of well-dated, manufactured items, archaeologists might use these materials to date archaeological remains rather than radiocarbon ages from organic remains. This potentially occurs in N. America after European Colonial activity because European manufactured items can often be dated precisely. It is also a potential problem in the US Southwest

where painted ceramics can be used to date archaeological sites (71). Thus, one potential issue is that declines in radiocarbon frequency near the end of a N. American sequence (e.g., 400 cal BP) may be due to a lack of samples rather than a "real drop" in population and economic activity. To blunt the impact of a potential edge effect from sampling bias late in time, we calibrated and constructed KDEs and SPDs until 200 cal BP. We then trimmed these back to 410 cal BP, eliminating post 410 cal BP portions of the radiocarbon probability distributions. More importantly, independent lines of evidence indicate that the large drop in population that we observe in the Middle Mississippi River Valley about 800 cal BP is not a simple artifact of a lack of sampling. For instance, the DINAA database indicates a population decline in the Midwest and Middle Mississippi River valley from 780 to 400 cal BP (78–80). This corresponds with the decline in radiocarbon frequency and occurs 300-400 years before any European items useful to date archaeological remains appear. Further, as discussed in the manuscript, changes in isotope data and carbohydrate production track the population decline in both regions, indicating real changes toward less carbohydrate production in both regions as the carrying capacity of the systems declined.

Finally, one point of our model is to explain variability in where we observe large recessions. More prolonged growth follows from innovations that result in larger productivity gains, but make a system vulnerable to larger overshoots. We observe a much less severe recession in Texas where populations intensified their production of wild plants than in the Middle Mississippi River Valley where populations intensified on maize and local domesticates, fueling large political economies. It is not clear how edge effects would produce this pattern since both regions experienced European colonialism at about the same time, and one would need to engage in post hoc reasoning to accommodate the differences in recession to edge effects. That is, one would need to speculate on why archaeologists in Texas use radiocarbon dating more than archaeologists in Illinois and Missouri later in time. Such speculation seems unwarranted, especially when one considers that radiocarbon date frequencies actually increase from 500 to about 200 cal BP in the Middle Mississippi River Valley.

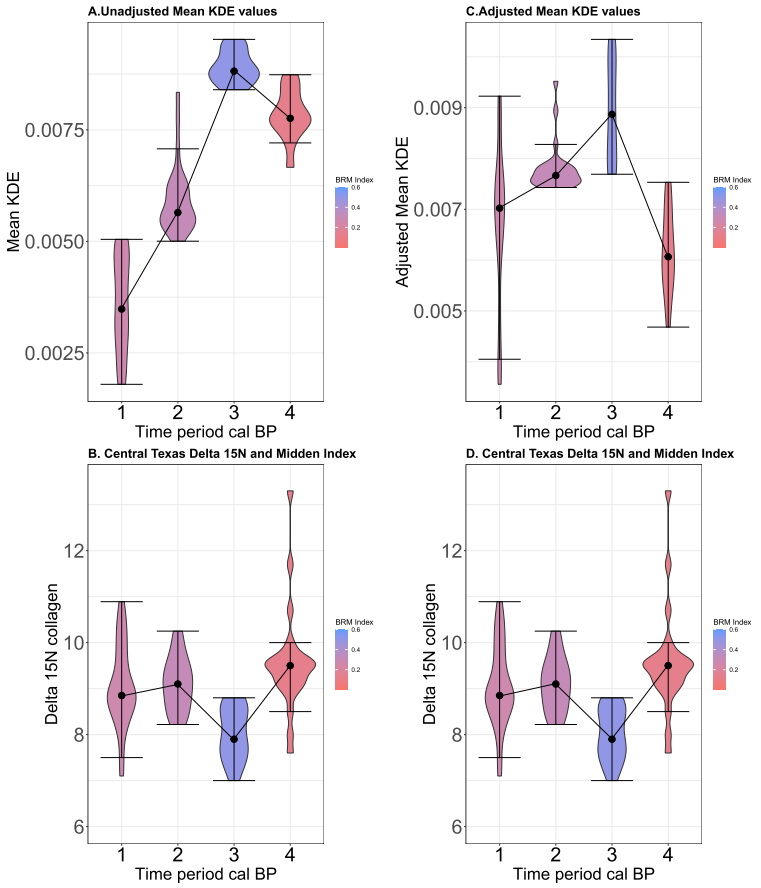

Fig. S11. A-Violin plots of population density by cultural historical time periods in Central Texas as estimated by mean kernel density estimates (KDE). B-Violin plots of $\delta\,^{15}N$ values by cultural historical time periods. C-Violin plots of population density estimates by cultural historical time period for a mean KDE adjusted for taphonomic loss following (81). D-Violin plots of $\delta\,^{15}N$ values by cultural historical time periods. In all graphs, the change in color of the violin plots indicates changing technology over time from less (red) to more to intensive carbohydrate processing (blue) technology. In this case, the ratio of large burned rock features to all (large + small) burned rock features.

Taphonomy. In archaeology, taphonomy refers to the processes by which the byproducts of human activity become preserved as traces of past systems. One of our anonymous reviewers served as a helpful skeptic of our work, and proposed in their review that the population expansion observed over 3,000 years in the case studies may be due to taphonomic loss. There are two issues: (1) Archaeological radiocarbon may simply increase over time because older sediments that hold archaeological

remains are less prevalent in the contemporary world than younger sediments (81–84). This idea proposes that the ability of archaeologists to sample organic remains that are traces of past systems is not determined by the size of past human systems but, instead, by the availability of preserved archaeological remains. This is a hypothesis based on a model of the loss of sediments over time that we call the Taphonomic Loss Hypothesis (81, 83, 84). (2) A second issue is whether a proposed global model of taphonomic adjustment is appropriate to apply across cases when conducting a comparison of the population dynamics of multiple cases.

Issue 1: Population expansion is simply due to a loss of sample space. In principle, it is possible that the taphonomic process of sediment loss impacts the distributions of archaeological radiocarbon (81, 83, 84). At this point, however, we believe this argument is better warranted for the terminal Pleistocene and early Holocene than it is for the Middle and Late Holocene. This point has been supported in recent scholarship that has revised the original, global taphonomic adjustment function (81). To investigate this possibility more, we followed the advice of one of our anonymous reviewers and created Figs. S11 and S12 for Central Texas and the Middle Mississippi River Valley. These Figs. compare median population density estimates and changes in resource production and consumption for an unadjusted mean KDE (used in the main text) and a mean KDE adjusted for taphonomic loss.

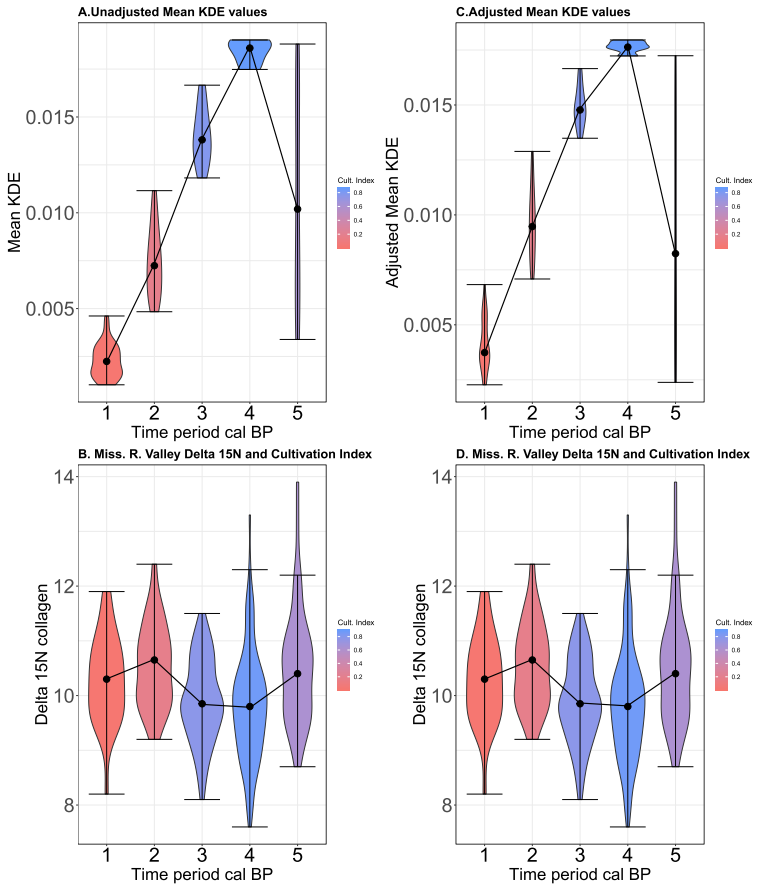

Fig. S12. A-Violin plots of population density by cultural historical time periods in the Middle Mississippi River Valley as estimated by mean kernel density estimates (KDE). B-Violin plots of $\delta\,^{15}N$ values by cultural historical time periods. C-Violin plots of population density estimates by cultural historical time period for a mean KDE adjusted for taphonomic loss following (81). D-Violin plots of $\delta\,^{15}N$ values by cultural historical time periods. In all graphs, the change in color of the violin plots indicates changing technology over time from less (red) to more to intensive carbohydrate processing (blue) technology. In this case, the ratio of domesticated seeds to nuts (i.e., nuts + domesticates).

For example, Fig. S11 compares the change in estimated population density by cultural historical time periods with changes in resource production and consumption in Central Texas. Fig. S11A and B simply replicate the results in the main text. The increase in population density from period 1 to 3 (3,500 to 650 cal BP) associates with increases in the intensive production of roots and bulbs in earth ovens (higher midden ratio) and a drop in nitrogen values during the period of peak population density. Fig. S11C and D replicate A and B, except that in this comparison we attempt to adjust for the potential loss of radiocarbon ages using a global taphonomic adjustment function (81). The key question is: Does the adjustment of the KDEs change our interpretation that population expanded from 3,500 to 800 cal BP in association with changes in resource production and consumption? No. Even the adjusted mean KDE displays period-by-period increases in population density. These increases in population density estimates associate with increases in the intensive production of roots and bulbs and lower protein consumption during the period of peak population density. We note two additional patterns: (a) Taphonomic adjustment

creates much more variability during period 1 in population density estimates, and (b) the taphonomic adjustment amplifies population decline during period 4. For now, the point remains that population expansion occurs in both the unadjusted and adjusted mean KDEs, and these patterns are consistent with our model that changes in resource production drive long-term population expansion.

Fig. S12 compares the change in estimated population density by cultural historical time periods with changes in in resource production and consumption in the Middle Mississippi River Valley. Again, Fig. S12A and B replicate the results in the main text. The increase in population density over 3,000 years associates with increases in the intensive production of domesticates and a drop in nitrogen values during the period of peak population density. Fig. S12C and D replicate A and B, except that in this comparison we attempt to adjust for the potential loss of radiocarbon ages using a global taphonomic adjustment (81). As above, the fundamental pattern does not change. From cultural historical periods 1 to 4, population density expanded. The increase in population density over time associates with increases in the intensive production of domesticates and a drop in nitrogen values during the period of peak population density (period 4). Moreover, the pattern of population expansion is also evidenced in site counts between 4,000 and 500 cal BP (85, p. 31-32). During cultural historical periods 3 and 4, the archaeological record in the Mississippi River Valley and the Eastern Woodlands more generally indicate the widespread occupation of villages, the emergence of ceremonial centers, and urban like settlements with platform mounds and plazas (85, p. 96, 100-101, 113). These data also suggest that population expansion occurred. In short, the patterns of population expansion and changes in resource production are consistent with our hypothesis that changes in resource production drove long-term changes in population.

In summary, the Tahponomic Loss Hypothesis needs more investigation. It is possible that over the last 20,000 years cal BP, it is increasingly difficult to detect signals of past population dynamics from large samples of archaeological radiocarbon during the Early Holocene and Late Pleistocene. However, as noted below, taphonomic loss is less of an issue during the Late Holocene, a point emphasized in our core case studies by the fact that taphonomic adjustment does not change the underlying interpretation of population expansion from 3,500 to 800 cal BP. Further, multiple lines of evidence indicate population expansion in the Middle Mississippi River Valley. Interestingly, the global taphonomic adjustment leads to increased variability in population density estimates during period 1 of both core case studies and a sharper decline in the median population density estimate during the final period of both core case studies.

Issue 2: Global taphonomic adjustment and uncertainty in cross-case comparisons. As it stands, the work by (81, 83, 84) has led, to use Timpson's term (86), to a "misunderstanding": One can use a global power function that describes the loss of sediments to adjust SPDs or KDEs to represent the "true" dynamics of past human populations. However, the proposed procedure to adjust for taphonomy introduces complexity and uncertainty into the underlying data, and this can reduce the ability of researchers to interpret the adjusted records and, critically, make comparisons between records. This occurs for three reasons.

First, the most recent power function (used above) (81) is:

$$l = 21149.57(t + 1788.03)^{-1.26}. \quad [1]$$

Where l is the loss of datable contexts, t is time, and the other values are parameters that determine the shape of the power function. The parameters above are derived from fitting a regression model of time against the loss of sediments in two global data sets argued not impacted by humans. However, there is considerable uncertainty about the values of these parameters across geomorphic contexts (e.g., 87). The sequences we analyze are drawn from large areas, which contain many kinds of depositional environments. Some of these environments may experience high rates of loss of preserved carbon, while others may preserve discarded carbon at high rates. Indeed, Bluhm and Surovell find that even in the two global databases that they use, the uncertainty of parameter estimates increases after 6,000 cal BP and especially after 2,000 cal BP (81). This is one reason why researchers should have a good a prior justification for applying a taphonomic adjustment (88), especially when analyzing time-series covering the last 6,000 years. Recent work by Contreras and Codding (89) supports this point. Contreras and Codding propose the development of local taphonomic adjustments to overcome spurious peaks and troughs created by global scale adjustments in local SPDs/KDEs. However, they also note that local scale adjustments have to be accurate to approximate real population trajectories. Because of the lack of local scale adjustments and the outstanding problems in developing accurate local scale adjustments, and the fact that we are comparing different geomorphic regions in this paper, we believe it is better to not use a taphonomic adjustment. Without local scale taphonomic adjustments for each of our study regions, a more conservative approach that induces less noise is the appropriate method.

Second, the taphonomic adjustment model above assumes that taphonomic processes only result in deletion. This is not a fair assumption. For example, the fire-cracked rock midden landscapes in Central Texas trapped ever more archaeological remains as people accumulated these middens. Mississippian and Late Woodland villages are features on top of features (e.g., 10,000+ features in 1 ha is not uncommon in floodplains). This environmental modification generates human made geological features (e.g., tells in the Levant, Maya Mounds, burned rock middens, etc.) that preserve more and more archaeological remains for archaeologists to dig-up and date. Most of the radiocarbon ages in the data sets that we use come from excavation contexts. Thus, it is likely that the larger taphonomic process over the last 3,000 years is human modifications of the environment that lead to accumulations of more readily preserved archaeological remains and more organic remains available for dating during excavations. Using a taphonomic adjustment in such a situation, again, adds complexity and uncertainty to the interpretation of the underlying data.

Third, the correlation of multiple proxies of population change suggest that archaeological radiocarbon is useful to detect the signals of population growth that occurred in the past (e.g., 71, 75–77). For example, as discussed above, multiple lines of

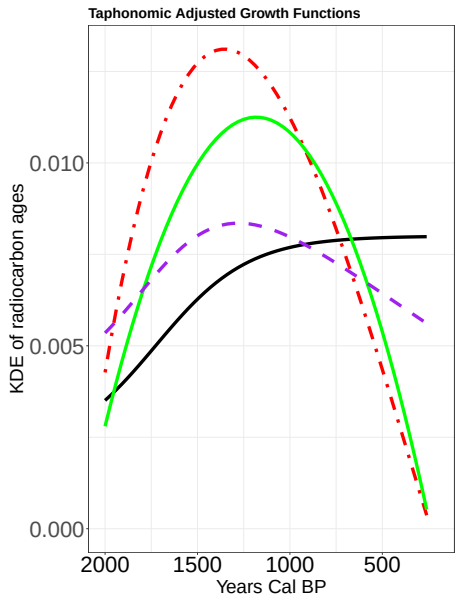

Fig. S13. The effect of taphonomic adjustment on an inverse U shaped underlying population signal (green curve) and a logistic population signal (black curve). The red and purple dashed curves illustrate the effect of taphonomic adjustment on the shapes of the curves. Taphonomic adjustment modifies the shapes of the curves.

evidence indicate a population expansion, at least since 2,000 cal BP and a decline from about 780 to 500 cal BP (Periods 3-5) in the Middle Mississippi River Valley (see above and (85)). This suggests that archaeological radiocarbon is detecting a real signal of relative changes in population size shaped like an inverse U over time (2,000-500 cal BP). As such, the taphonomic adjustment model entails dividing a known non-linear process (the inverse U population signal) by another known non-linear process (the taphonomic adjustment function). Fig. S13 illustrates the consequence of dividing a known inverse U shaped curve by the global taphonomic adjustment. Note how the adjusted curve (red dashed curve) now peaks before the unadjusted curve, the peak is higher, and the decline is steeper. In this case, we have independent data suggesting that the population signal is an inverse U, so we can interpret the effect of the taphonomic adjustment. However, across cases, this is not necessarily the case. For instance, the black curve in Fig.S13 illustrates the simple case in which we suppose that a population changed according to a logistic distribution, approaching a carrying capacity over time (rather than an inverse U). We then apply the taphonomic adjustment to this distribution (purple curve). Dividing two non-linear functions (the logistic and the taphonomic power function) "adjusts" the interpretation. Under taphonomic adjustment the population has a peak at about 1,200 and then displays a crash.

The net result of all three points above is that a global taphonomic adjustment likely makes comparing archaeological radiocarbon time-series across cases more difficult, and, at least in our cases, it does not appear to lead to more faithful representations of past population dynamics but to more complex representations across cases. In our main analysis, we have, thus, been conservative and not used a global taphonomic adjustment.

Part III: ArchaeoGlobe Data and Analysis

As with the case studies discussed above, we estimated the population dynamics of eight archaeoGlobe regions using mean KDEs and SPDs smoothed at 100 year intervals. We constructed all KDEs in these regions using 200 simulations and a bandwidth of 50. We then calculated the mean KDE and summed the mean KDEs into 30 year bins. These procedures smooth the KDEs to capture the long-term trend over time and reduce intra-generational fluctuations over shorter time-scales induced by calibration and/or biases introduced by site over-sampling. We used Intcal2020 to calibrate the radiocarbon ages (90).

Fig. S14 illustrates the the mean KDEs and simulated KDEs used to estimate long-term population growth in each ArchaeoGlobe region. In all eight cases, we ran simulated KDEs from 3,500 to 200 cal BP and then trimmed the resulting KDEs back to 410 cal BP. We did this to cope with suspected sample bias after 410 cal BP in North America. After this time, often historic artifacts can be used to date archaeological sites, and this decreases the number of radiocarbon ages analyzed. The mean KDEs seem to support this idea, with many of the KDEs displaying negative growth rates that accelerate after 380 cal BP.

Fig. S14 illustrates some of the main patterns discussed in the paper. In the Southwest (SW), Midwest (MW), Southeast (SE), and Rocky Mountain (RM) regions, the mean KDE overshoots the logistic model by a lot. However, in the Western region (WE), there is no overshoot that appears distinct from earlier fluctuations around the logistic model. As discussed above, we do not consider the overshoots and recessions near the end of these sequences as edge effects. This is because the recessions occur too early and independent lines of evidence also indicate population recessions.

For instance, Robinson et al. 2021 illustrate that the recession in the US Southwest (Fig. S14A) at 800 cal BP occurs in the

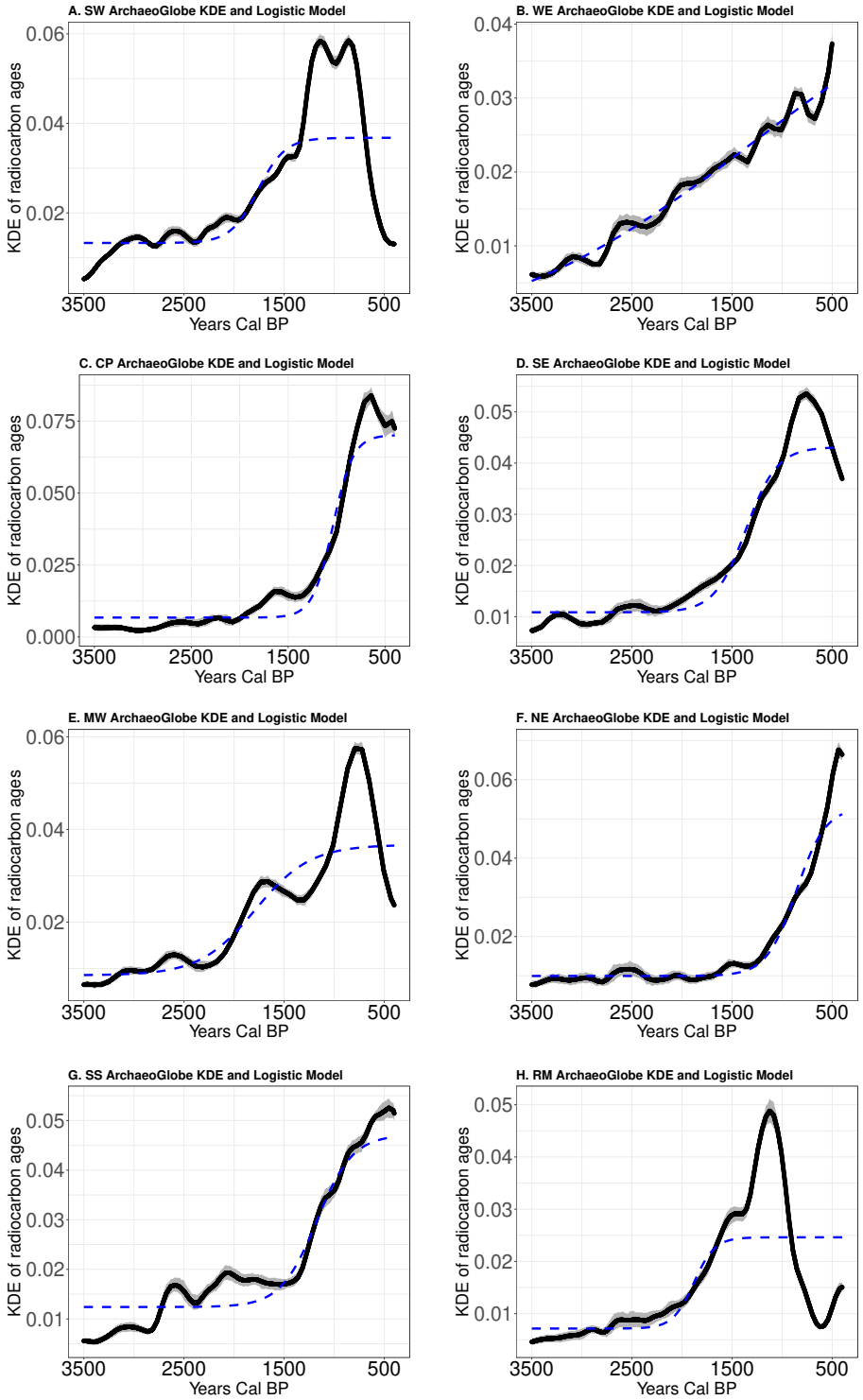

Fig. S14. Mean KDE and 95% confidence envelope of simulated KDEs (grey shading), and logistic models (dashed blue curves) fit to each ArchaeoGlobe region. SW=US Southwest, WE=Western US; CP=US Central Plains; SE=Southeast US; MW=Midwest US; NE=Northeast US; SS= Southern Central US Plains; RM=US Rocky Mountains. See Fig. 2 in the main text for a map that delineates each region.

radiocarbon data set, a tree ring data set (cuttings can be used as a proxy for building activity), and a pueblo structure count data set (71). As discussed above, the DINAA database also indicates a large population decline in the Midwest (MW) from 780 to 400 cal BP (78–80). This database consists of sites and components of sites and tracks the frequency of site components, many dated relatively (i.e, through materials associated with known manufacture dates), over time (78–80), and shows that site components change spatially and become much less frequent, especially around the Middle Mississippi River Valley. In general, in the regions where we do observe large recessions near the end of the sequence all occur well before 410 cal BP, (800 cal BP in the Southwest, 780 cal BP in the Midwest, 680 cal BP in the Southeast, and 1,000 cal BP in the Rocky Mountains). These large recessions occur well before other relative dating techniques become widely available. Indeed, the US Southwest provides an interesting test case. Pottery sequences tied to tree ring ages have long been used for dating sites postdating 1,400 cal BP in this region. This is cheaper and easier in many contexts than radiocarbon dating. Yet, the radiocarbon frequency still tracks the population recession at 800 cal BP rather than beginning when painted pots appear in the archaeological record and archaeologists use them for dating purposes circa. 1,400 cal BP (71).

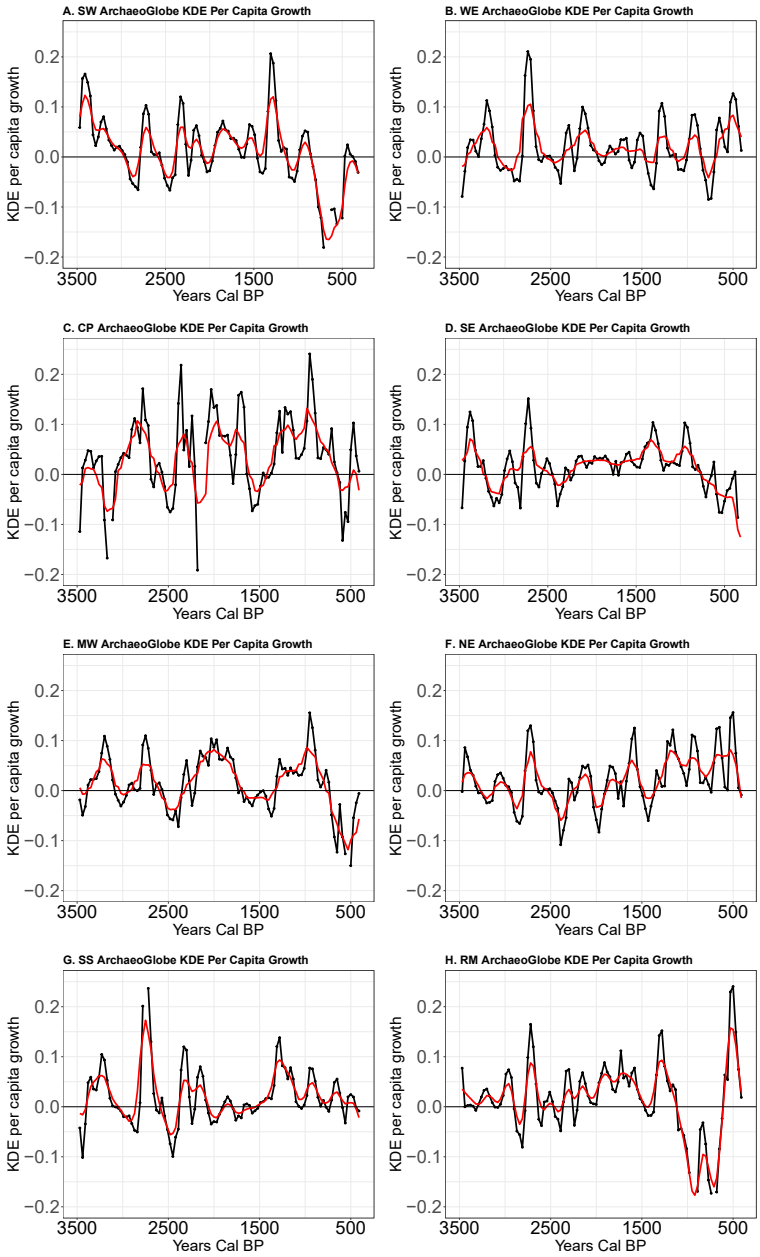

Fig. S15. *Per capita* growth rates of SPDs with a 100 year smoothing mean (black line) and mean KDE (red line). Both the SPD and mean KDE are summed by 30 year generations. SW=US Southwest, WE=Western US; CP=US Central Plains; SE=Southeast US; MW=Midwest US; NE=Northeast US; SS= Southern Central US Plains; RM=US Rocky Mountains. See Fig. 2 in the main text for a map that delineates each region.

Fig. S15 illustrates *per capita* growth rates of each ArchaeoGlobe region over time for both the mean KDE and SPDs calculated for each region. As noted above, the SPD displays more variability than the mean KDEs in all of the regions. These graphs allow us to count the number of consecutive generations that a region experienced positive or negative *per capita* growth and the maximum or minimum growth value in any given period of growth or decline.

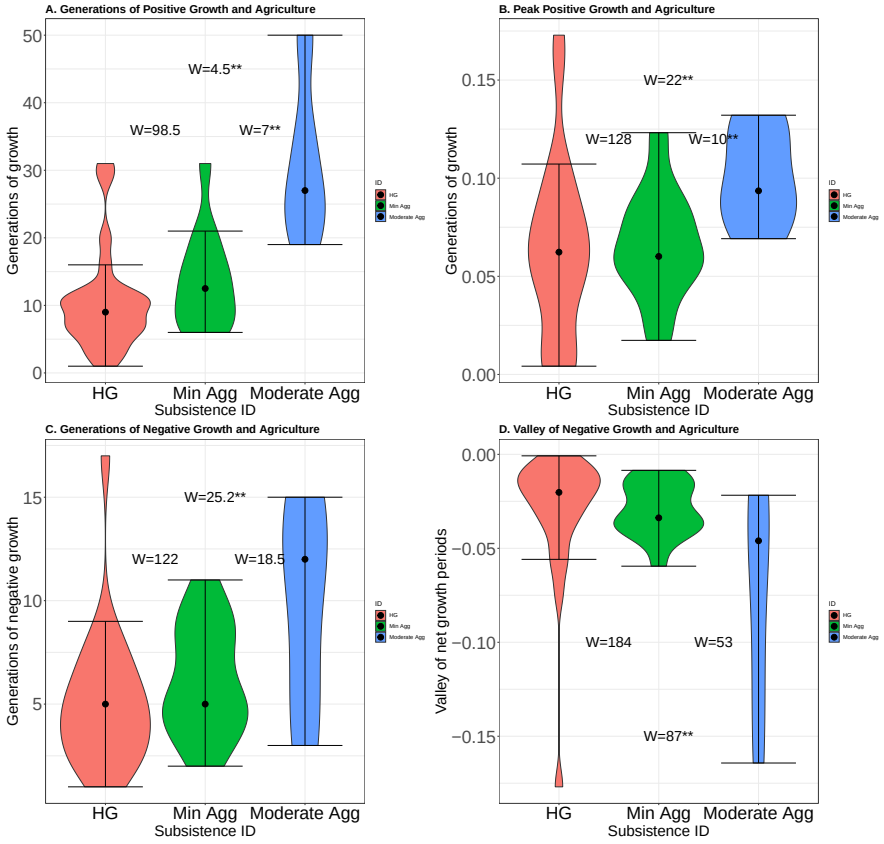

Fig. S16. A-Generations of consecutive positive *per capita* growth rates among ArchaeoGlobe regions by subsistence land use categories. B-Peak *per capita* growth during periods of positive growth. C-Generations of consecutive negative *per capita* growth rates among ArchaeoGlobe regions by subsistence land use categories. D-The lowest *per capita* growth rate associated with periods of negative growth in the eight ArchaeoGlobe regions. In all graphs, HG=hunting, gathering, and fishing. Min. Agg=extensive agriculture only. Moderate Agg.= extensive and intensive agriculture land use types.

Fig. S16 summarizes the results of our analysis of the mean KDE of the length of consecutive growth and decline periods by land use categories documented in ArchaeoGlobe. To capture differences in land use, we coded each case and 1000 year time period as HG=hunting and gathering land us only, Minimum Agg.=the presence of extensive agriculture; Moderate Agg.=the presence of extensive and intensive agricultural land use. Fig. S16 expands on Fig. 3 in the main paper and illustrates that as land use shifts toward intensive agriculture, the length of positive growth periods increases and the intensity or maximum *per capita* growth increases. Similarly, as land use shifts toward intensive agriculture, periods of negative *per capita* growth become longer and more intense. If we analyze the SPDs instead of the KDEs, these patterns simply become stronger. We use the mean KDEs here to error on the conservative side, in terms of identifying false short term fluctuations.

References

1. JM Anderies, Culture and human agro-ecosystem dynamics: The Tsembaga of New Guinea. *J. Theor. Biol.* **192**, 515–530 (1998).
2. J Freeman, RP Mauldin, M Whisenhunt, RJ Hard, JM Anderies, Repeated long-term population growth overshoots and recessions among hunter-gatherers. *The Holocene* **33**, 1163–1175 (2023).
3. L Tieszen, T Fagre, Effect of diet quality and composition on the isotopic composition of respiratory CO^2, bone collagen, bioapatite, and soft tissues in *Prehistoric Human Bone–Archaeology at the Molecular Level*, eds. J Lambert, G Grupe. (Coastal Archaeological Research, Corpus Christi, TX), pp. 121–125 (1993).
4. GD Farquhar, JR Ehleringer, KT Hubick, Carbon isotope discrimination and photosynthesis. *Annu. Rev. Plant Biol.* **40**, 503–537 (1989).
5. MH O'Leary, Carbon isotopes in photosynthesis. *Bioscience* **38**, 328–336 (1988).
6. J Ehleringer, T Cerling, c_3 and c_4 photosynthesis in *Encyclopedia of Global Environmental Change, vol. II.*, eds. H Mooney, J Canadell. (John Wiley and Sons, London), pp. 186–190 (2001).

7. JR Ehleringer, TE Cerling, BR Helliker, c_4 photosynthesis, atmospheric co^2, and climate. *Oecologia* **112**, 285–299 (1997).
8. LL Tieszen, Stable isotopes on the Plains: Vegetation analyses and diet determinations in *Skeletal Biology in the Great Plains: Migration, warfare, health, and subsistence*, eds. DW Owsley, RL Jantz. (Smithsonian Institution, Washington, D.C.), pp. 261–289 (1994).
9. MJ Kohn, Carbon isotope compositions of terrestrial c_3 plants as indicators of (paleo) ecology and (paleo) climate. *Proc. Natl. Acad. Sci.* **107**, 19691–19695 (2010).
10. Z Sharp, *Principals of Stable Isotope Geochemistry*. (Pearson Education, Upper Saddle River, NJ), (2007).
11. R Tykot, Stable isotopes and diet: You are what you eat in *Proceedings of the International School of Physics "Enrico Fermi" Course CLIV*, eds. M Milazzo, M Piacentine. (IOS Press, Amsterdam), pp. 433–444 (2004).
12. P Deines, The isotopic composition of reduced organic carbon in *Handbook of Environmental Isotope Geochemistry*, eds. P Fritz, J Fontes. (Elsevier, Amsterdam), pp. 329–406 (1980).
13. MH O'Leary, Carbon isotope fractionation in plants. *Phytochemistry* **20** (1981).
14. T Boutton, Stable carbon isotope ratios of natural materials: II. atmospheric, terrestrial, marine, and freshwater environments. in *Carbon Isotope Techniques*, ed. B Coleman, D.C.and Fry. (Academic Press, Inc., Burlington), pp. 173–185 (1991).
15. MJ DeNiro, Stable isotopy and archaeology. *Am. scientist* **75**, 182–191 (1987).
16. W Cockburn, Variation in photosynthetic acid metabolism in vascular plants: Cam and related phenomena. *New Phytol* **101**, 3–24 (1985).
17. WG Eickmeier, MM Bender, Carbon isotope ratios of crassulacean acid metabolism species in relation to climate and phytosociology. *Oecologia* **25**, 341–347 (1976).
18. H Bocherens, D Drucker, Trophic level isotopic enrichment of carbon and nitrogen in bone collagen: case studies from recent and ancient terrestrial ecosystems. *Int. J. Osteoarchaeol.* **13**, 46–53 (2003).
19. SH Ambrose, MJ DeNiro, The isotopic ecology of East African mammals. *Oecologia* **69**, 395–406 (1986).
20. MJ DeNiro, S Epstein, Influence of diet on the distribution of nitrogen isotopes in animals. *Geochimica et Cosmochimica Acta* **45**, 341–351 (1981).
21. A Mariotti, Atmospheric nitrogen is a reliable standard for natural ^{15}n abundance measurements. *Nature* **303**, 685–687 (1983).
22. SH Ambrose, Effects of diet, climate and physiology on nitrogen isotope abundances in terrestrial foodwebs. *J. Archaeol. Sci.* **18**, 293–317 (1991).
23. G Shearer, DH Kohl, n_2-fixation in field settings: Estimations based on natural ^{15}n abundance. *Funct. Plant Biol.* **13**, 699–756 (1986).
24. JW Oakley, J Simons, GW Stunz, Spatial and habitat-mediated food web dynamics in an oyster-dominated estuary. *J. Shellfish. Res.* **33**, 841–855 (2014).
25. B Wissel, B Fry, Tracing Mississippi River influences in estuarine food webs of coastal louisiana. *Oecologia* **144**, 659–672 (2005).
26. B Fry, Food web structure on Georges Bank from stable C, N, and S isotopic compositions. *Limnol. Oceanogr.* **33**, 1182–1190 (1988).
27. M Minagawa, E Wada, Stepwise enrichment of ^{15}n along food chains: further evidence and the relation between $\delta!^{15}n$ and animal age. *Geochimica et cosmochimica acta* **48**, 1135–1140 (1984).
28. BS Chisholm, DE Nelson, HP Schwarcz, Stable-carbon isotope ratios as a measure of marine versus terrestrial protein in ancient diets. *Science* **216**, 1131–1132 (1982).
29. M Katzenberg, Stable isotope analysis: a tool for studying past diet, demography and life history in *Biological Anthropology of the Human Skeleton, second Ed.*, eds. A Katzenberg, M Saunders, R Shelley. (Wiley-Liss, John Wiley and Sons, Inc., New York), pp. 413–441 (2008).
30. SH Ambrose, L Norr, Evidence for the relationship of the carbon isotope ratios of whole diet and dietary protein to those of bone collagen and carbonate in *Prehistoric Human Bone: Archaeology at the Molecular Level*, eds. JB Lambert, B Grupe. (Springer-Verlag, Berlin, Germany), pp. 1–37 (1993).
31. S Ambrose, L Norr, Experimental evidence for the relationship of the carbon isotope ratios of whole diet and dietary protein to those of bone collagen and carbonate in *Prehistoric Human Bone-archaeology at the Molecular Level*, eds. J Lambert, G Grupe. (Springer-Verlag, Berlin), pp. 1–37 (1993).
32. AW Froehle, CM Kellner, MJ Schoeninger, Focus: effect of diet and protein source on carbon stable isotope ratios in collagen: follow up to warinner and tuross (2009). *J. Archaeol. Sci.* **37**, 2662–2670 (2010).
33. CM Kellner, MJ Schoeninger, A simple carbon isotope model for reconstructing prehistoric human diet. *Am. J. Phys. Anthropol.* **133**, 1112–1127 (2007).
34. JA Lee-Thorp, JC Sealy, NJ Van Der Merwe, Stable carbon isotope ratio differences between bone collagen and bone apatite, and their relationship to diet. *J. archaeological science* **16**, 585–599 (1989).
35. CH Sullivan, HW Krueger, Carbon isotope analysis of separate chemical phases in modern and fossil bone. *Nature* **292**, 333–335 (1981).
36. S Jim, V Jones, SH Ambrose, RP Evershed, Quantifying dietary macronutrient sources of carbon for bone collagen biosynthesis using natural abundance stable carbon isotope analysis. *Br. J. Nutr.* **95**, 1055–1062 (2006).
37. S Jim, SH Ambrose, RP Evershed, Stable carbon isotopic evidence for differences in the dietary origin of bone cholesterol,

collagen and apatite: implications for their use in palaeodietary reconstruction. *Geochimica et Cosmochimica Acta* **68**, 61–72 (2004).
38. SH Ambrose, BM Butler, DB Hanson, RL Hunter-Anderson, HW Krueger, Stable isotopic analysis of human diet in the Marianas Archipelago, Western Pacific. *Am. J. Phys. Anthropol. The Off. Publ. Am. Assoc. Phys. Anthropol.* **104**, 343–361 (1997).
39. GR Milner, JL Boldsen, Population trends and the transition to agriculture: Global processes as seen from north america. *Proc. Natl. Acad. Sci.* **120**, e2209478119 (2023).
40. TE Emerson, KM Hedman, ML Simon, MA Fort, KE Witt, Isotopic confirmation of the timing and intensity of maize consumption in greater cahokia. *Am. Antiq.* **85**, 241–262 (2020).
41. GR Milner, JL Boldsen, Population trends and the transition to agriculture: Global processes as seen from north america, supporting information appendix, section 3 archaeobotanical data. *Proc. Natl. Acad. Sci.* **120**, e2209478119 (2023).
42. R Boyd, PJ Richerson, *The origin and evolution of cultures*. (Oxford University Press), (2004).
43. RP Mauldin, DL Nickels, Burned rock middens in Texas in *Archaeological Testing to Determine the National Register Eligibility Status of 18 Prehistoric Sites on Camp Bowie, Brown County, Texas, Volume 1*, eds. RP Mauldin, D Nickels, C Broehm. (Archaeological Survey Report No. 334, The Center for Archaeological Research. TxDOT-ENV Archeological Studies Program, Report No. 134. The University of Texas at San Antonio, San Antonio, TX), pp. 217–231 (2003).
44. SL Black, DG Creel, The Central Texas burned rock midden reconsidered in *Hot Rock Cooking on the Greater Edwards Plateau: Four Burned Rock Midden Sites in West Central Texas*, eds. SL Black, LW Ellis, DG Creel, GT Goode. (Studies in Archeology 22. Texas Archeaological Research Laboratory, The University of Texas at Austin, Austin, TX), pp. 269–301 (1997).
45. SL Black, AV Thorns, Hunter-gatherer earth ovens in the archaeological record: fundamental concepts. *Am. Antiq.* **79**, 204–226 (2014).
46. AV Thoms, The fire stones carry: ethnographic records and archaeological expectations for hot-rock cookery in western North America. *J. Anthropol. Archaeol.* **27**, 443–460 (2008).
47. AV Thoms, Rocks of ages: propagation of hot-rock cookery in western North America. *J. Archaeol. Sci.* **36**, 573–591 (2009).
48. SL Black, Research module 2: Studying the hearths of the greater Edwards Plateau in *Pavo Real (41BX52): A Paleoindian and Archaic Camp and Workshop on the Balcones Escarpment, South-Central Texas*, eds. DR Collins, Michael B. Hudler, SL Black. (Studies in Archeology 41. Texas Archaeological Research Laboratory, The University of Texas at Austin, Austin, TX), pp. 375–405 (2003).
49. RP Mauldin, DL Nickels, CJ Broehm, *Archaeological Testing to Determine the National Register Eligibility Status of 18 Prehistoric Sites on Camp Bowie, Brown County, Texas, Archaeological Survey Report No. 334*. (Center for Archaeological Research, The University of Texas at San Antonio, San Antonio, TX), (2003).
50. LW Ellis, Hot rock technology in *Hot Rock Cooking on the Greater Edwards Plateau: Four Burned Rock Midden Sites in West Central Texas*, eds. SL Black, LW Ellis, DG Creel, GT Goode. (Studies in Archeology 22. Texas Archaeological Research Laboratory, The University of Texas at Austin, Austin, TX), pp. 43–81 (1997).
51. RT Stark, Ph.D. thesis (PhD Thesis, Department of Anthropology, University of Texas, Austin) (2002).
52. P Dering, Earth-oven plant processing in Archaic period economies: An example from a semi-arid savannah in south-central North America. *Am. Antiq.* **64**, 659–674 (1999).
53. L Wandsnider, The roasted and the boiled: food composition and heat treatment with special emphasis on pit-hearth cooking. *J. anthropological archaeology* **16**, 1–48 (1997).
54. AV Thoms, Ph.D. thesis (PhD Thesis, Department of Anthropology, Washington State University, Pullman) (1989).
55. W Buskirk, *The Western Apache*. (University of Oklahoma Press, Norman, OK), (1987).
56. EF Castetter, ME Opler, *The Ethnobiology of the Chiricahua and Mescalero Apache: The Use of Plants for Foods, Beverages, and Narcotics*. (Ethnobiological Studies in the American Southwest, vol. III. The University of New Mexico Bulletin 4(5). University of New Mexico Press, Albuquerque, NM), (1936).
57. R McAuliffe, RP Mauldin, SL Black, Central Texas plant baking in *Earth Ovens and Desert Lifeways: 10,000 Years of Indigenous Cooking in the Arid Landscapes of North America*, eds. CW Koenig, MR Miller. (University of Utah Press, Salt lake City, UT), pp. 33–60 (2022).
58. L Acuña, Master's thesis (Master's Thesis, Department of Anthropology, Texas State University, San Marcos) (2006).
59. PJ Dering, Appendix C: Botanical perspectives on land use in the cross timbers and prairies in *Archaeological Testing to Determine the National Register Eligibility Status of 18 Prehistoric Sites on Camp Bowie, Brown County, Texas, Volume 2*, eds. RP Mauldin, D Nickels, C Broehm. (Archaeological Survey Report No. 334, The Center for Archaeological Research. TxDOT-ENV Archeological Studies Program, Report No. 134. The University of Texas at San Antonio, San Antonio, TX), pp. 58–78 (2003).
60. PJ Dering, Appendix B: Plant remains from sites 41BR392, 41BR500, and 41BR522 located on Camp Bowie, Brown County, Texas in *Archaeological Testing of Four Sites on Camp Bowie, Brown County, Texas*, eds. JD Weston, RP Mauldin. (Center for Archaeological Research, University of Texas at San Antonio. Texas Antiquities Committee, Permit No. 2926, San Antonio, TX), pp. 98–108 (2003).
61. J Freeman, RJ Hard, RP Mauldin, JM Anderies, Radiocarbon data may support a Malthus-Boserup model of hunter-gatherer population expansion. *J. Anthropol. Archaeol.* **63**, 101321 (2021).

62. JD Weston, RP Mauldin, eds., *Archaeological Testing of Four Sites on Camp Bowie, Brown County, Texas.* (Archaeological Survey Report No. 335, Center for Archaeological Research University of Texas at San Antonio, San Antonio, TX), (2003).
63. SL Black, L Ellis, D Creel, G Goode, *Hot Rock Cooking on the Greater Edwards Plateau: Four Burned Rock Midden Sites in West Central Texas, 2 vols.* (Archaeological Research Laboratory and the Texas Department of Transportation, Austin, TX), (1997).
64. S Decker, Appendix J: Comparative data from excavated and reported burned rock middens in greater Central Texas in *Hot Rock Cooking on the Greater Edwards Plateau: Four Burned Rock Midden Sites in West Central Texas*, eds. SL Black, LW Ellis, DG Creel, GT Goode. (Studies in Archeology 22. Texas Archaeological Research Laboratory, The University of Texas at Austin, Austin, TX), pp. 683–745 (1997).
65. ER Crema, A Bevan, Inference from large sets of radiocarbon dates: software and methods. *Radiocarbon* **63**, 23–39 (2021).
66. J Wood, *The Biodemography of Subsistence Farming: Population, Food and Family.* (Cambridge University Press, Cambridge, UK) Vol. 87, (2020).
67. JW Wood, A theory of preindustrial population dynamics: Demography, economy, and well-being in Malthusian systems. *Curr. Anthropol.* **39**, 99–135 (1998).
68. PJ Richerson, R Boyd, RL Bettinger, Cultural innovations and demographic change. *Hum. biology* **81**, 211–235 (2009).
69. PJ Richerson, R Boyd, Homage to Malthus, Ricardo, and Boserup toward a general theory of population, economic growth, environmental deterioration, wealth, and poverty. *Hum. Ecol. Rev.* **4**, 85–90 (1998).
70. G Cowgill, On causes and consequences of ancient and modern population changes. *Am. Anthropol.* **77**, 505–525 (1975).
71. E Robinson, RK Bocinsky, D Bird, J Freeman, RL Kelly, Dendrochronological dates confirm a late prehistoric population decline in the American Southwest derived from radiocarbon dates. *Philos. Transactions Royal Soc. B* **376**, 20190718 (2021).
72. J Freeman, et al., Synchronization of energy consumption by human societies throughout the holocene. *Proc. Natl. Acad. Sci.* p. 201802859 (2018).
73. JW Rick, Dates as data: an examination of the peruvian preceramic radiocarbon record. *Am. Antiq.* pp. 55–73 (1987).
74. J Freeman, DA Byers, E Robinson, RL Kelly, Culture process and the interpretation of radiocarbon data. *Radiocarbon* **60**, 453–467 (2018).
75. SS Downey, E Bocaege, T Kerig, K Edinborough, S Shennan, The neolithic demographic transition in Europe: Correlation with juvenility index supports interpretation of the summed calibrated radiocarbon date probability distribution (scdpd) as a valid demographic proxy. *PloS one* **9**, e105730 (2014).
76. A Palmisano, D Lawrence, MW de Gruchy, A Bevan, S Shennan, Holocene regional population dynamics and climatic trends in the Near East: A first comparison using archaeo-demographic proxies. *Quat. Sci. Rev.* **252**, 106739 (2021).
77. K Edinborough, et al., Radiocarbon test for demographic events in written and oral history. *Proc. Natl. Acad. Sci.* **114**, 12436–12441 (2017).
78. GR Milner, G Chaplin, Eastern North American population at ca. AD 1500. *Am. Antiq.* **75**, 707–726 (2010).
79. GR Milner, DG Anderson, MT Smith, The distribution of Eastern Woodlands peoples at the prehistoric and historic interface in *Societies in Eclipse: Archaeology of the Eastern Woodland Indians, A.D. 1400-1700*, eds. DS Brose, CW Cowan, RCJ Manifort. (Smithsonian Institution Press, Washington D. C.), pp. 9–18 (2005).
80. DG Anderson, Examining prehistoric settlement distribution in eastern North America. *Archaeol. East. North Am.* pp. 1–22 (1991).
81. LE Bluhm, TA Surovell, Validation of a global model of taphonomic bias using geologic radiocarbon ages. *Quat. Res.* **91**, 325–328 (2019).
82. RL Kelly, TA Surovell, BN Shuman, GM Smith, A continuous climatic impact on Holocene human population in the Rocky Mountains. *Proc. Natl. Acad. Sci.* **110**, 443–447 (2013).
83. TA Surovell, J Byrd Finley, GM Smith, PJ Brantingham, R Kelly, Correcting temporal frequency distributions for taphonomic bias. *J. Archaeol. Sci.* **36**, 1715–1724 (2009).
84. TA Surovell, PJ Brantingham, A note on the use of temporal frequency distributions in studies of prehistoric demography. *J. Archaeol. Sci.* **34**, 1868–1877 (2007).
85. GR Milner, *The Moundbuilders: Ancient Societies of Eastern North America, Second Edition.* (Thames & Hudson, London), (2004).
86. A Timpson, *ADMUR: Ancient Demographic Modelling Using Radiocarbon* (University College London (UCL), Research Department of Genetics, Environment and Evolution (GEE), Darwin Building, Gower Street, London, WC1E 6BT), (2020).
87. JA Ballenger, JB Mabry, Temporal frequency distributions of alluvium in the American Southwest: taphonomic, paleohydraulic, and demographic implications. *J. Archaeol. Sci.* **38**, 1314–1325 (2011).
88. N Williams, Alan, The use of summed radiocarbon probability distributions in archaeology: a review of methods. *J. Archaeol. Sci.* **39**, 578 – 589 (2012).
89. DA Contreras, BF Codding, Landscape taphonomy predictably complicates demographic reconstruction. *J. Archaeol. Method Theory* pp. 1–27 (2023).
90. PJ Reimer, et al., The intcal20 northern hemisphere radiocarbon age calibration curve (0–55 cal kbp). *Radiocarbon* **62**, 725–757 (2020).